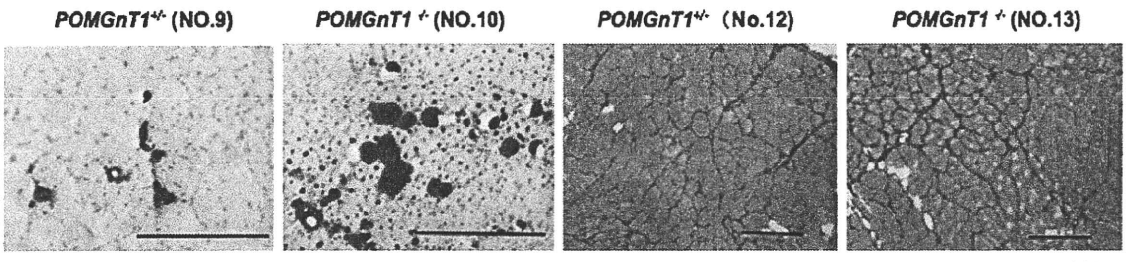

	genotype	sex	age	CTX interval(x3)	Fatty infiltration	Fibrosis
1	+/-	F	3M	2w	-	-
2	+/-	F	3M	2w	-	-
3	+/-	F	3M	2w	-~+	-~+
4	+/-	F	3M	2w	+	-~+
5	-/-	M	3M	2w	+	-~+
6	-/-	F	3M	2w	++	-~+
7	+/-	F	11M	1w	+	+
8	-/-	F	8.5M	1w	+	++
9	+/-	F	8.5M	1w	+	-~+
10	-/-	F	8.5M	1w	+~++	+~++
11	+/-	M	8.5M	1w	+	+
12	+/-	M	8.5M	1w	++	+
13	-/-	M	8.5M	1w	++	++

Fig. 6 – Impaired muscle regeneration of POMGnT1$^{-/-}$ mice. upper panel: representative Oil red O-stained or Sirius red-stained cross-sections of TA muscles of POMGnT1$^{-/-}$(−/−) and POMGnT1$^{+/-}$ (+/−) mice after three rounds of degeneration/regeneration evoked by cardiotoxin injection. One week after the last CTX injection, TA muscles were dissected, sectioned by a cryostat, fixed, and stained. lower table: Summary of fatty infiltration and fibrosis in regenerated muscles. CTX was injected into TA muscles three times with 2 weeks interval (2w) or 1 week interval (1w). The age at the first injection was shown. (−), well regenerated with minimal changes. (−~+), sporadic fatty regeneration or slight fibrosis between fibers. (+), mild fatty infiltration or mild fibrosis. (++), dense fatty infiltration or extensive fibrosis. F, female; M, male.

regulation of cell survival and proliferation. The levels of phosphorylation of these two kinases in POMGnT1$^{-/-}$ myoblasts were similar with those in wild-type myoblasts (Supplementary Fig. 1C). Consistent with these observations, TUNEL assay indicated that apoptosis is rare both in POMGnT1$^{-/-}$ and wild-type muscles (data not shown).

3. Discussion

In this study, we showed that in spite of mild muscle degeneration, the POMGnT1$^{-/-}$ satellite cells have much lower proliferative activity than wild-type satellite cells. The defect was not recovered by restoration of normal glycosylation of α-DG in mutant satellite cells. Together with the reduced sizes and the reduced numbers of myofibers of neonatal and adult POMGnT1$^{-/-}$ mice, these observations suggest that deficiency of POMGnT1 enzymatic activity impairs the functions of satellite cells.

3.1. *Two mouse models of muscle-eye-brain (MEB) disease*

Our POMGnT1$^{-/-}$ mice are the second mouse model of MEB disease. The first one was generated by gene trapping with a retroviral vector inserted into the second exon of the mouse POMGnT1 locus (Liu et al., 2006). As described in the literature, the phenotype is similar to ours with some differences. Our model shows much milder muscle phenotypes than the previously reported model, but also shows much a lower survival rate in the postnatal stage than the first model does. This would be due to more severe developmental abnormalities of the central nervous system of our mouse model, including disruption of the glia limitans, abnormal migration of neurons, and reactive gliosis in the cerebral cortex (manuscript in preparation), although these are also observed in the first model (Yang et al., 2007; Hu et al., 2007).

Mutation of the POMGnT1 gene is the cause of muscle–eye–brain disease (MEB) (Yoshida et al., 2001), which is characterized by severe congenital muscular dystrophy (Voit and Tome, 2004). Although glycosylation of α-DG was completely perturbed in our model, the POMGnT1$^{-/-}$ muscle showed only marginal pathological changes. Furthermore, POMGnT1$^{-/-}$ muscle showed normally formed muscle basal lamina on EM. These observations are in sharp contrast to the condition in humans. One possibility is that in the mouse, molecules other than α-DG are involved in the linkage of the sarcolemma with the extracellular matrix proteins, stabilizing the plasma membrane. As a candidate molecule, we examined β1-integrin expression in POMGnT1$^{-/-}$ muscle, but found that the level was not up-regulated. Therefore, the mechanism that explains this discrepancy remains to be clarified in a future study.

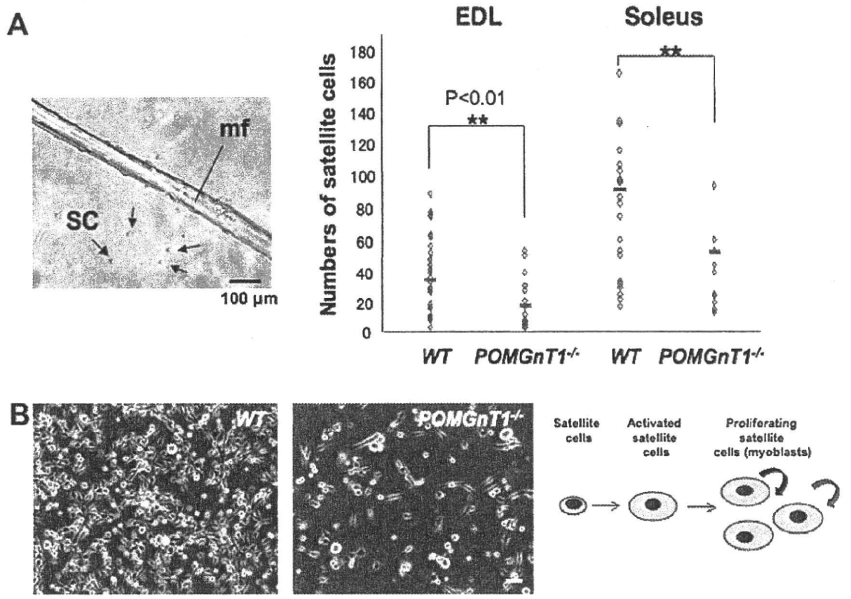

Fig. 7 – Activation and proliferation of satellite cells from WT and *POMGnT1*$^{-/-}$ mice. (A) Isolated myofibers were plated on Matrigel-coated 24 well-plates at one myofiber per well. Three days later, activated satellite cells (SC, arrows) around the parental fiber (mf) were counted and plotted. Small horizontal bars indicate the average number of activated/proliferating satellite cells originating from a myofiber from three independent experiments. Student's *t*-test. $^{**}p < 0.01$ (wild-type vs. *POMGnT1*$^{-/-}$ mice). (B) Satellite cells from WT and *POMGnT1*$^{-/-}$ mice 7 days after plating onto Matrigel-coated 24-well-plates at 2.5×10^3 cells/well. Scale bar, 100 μm.

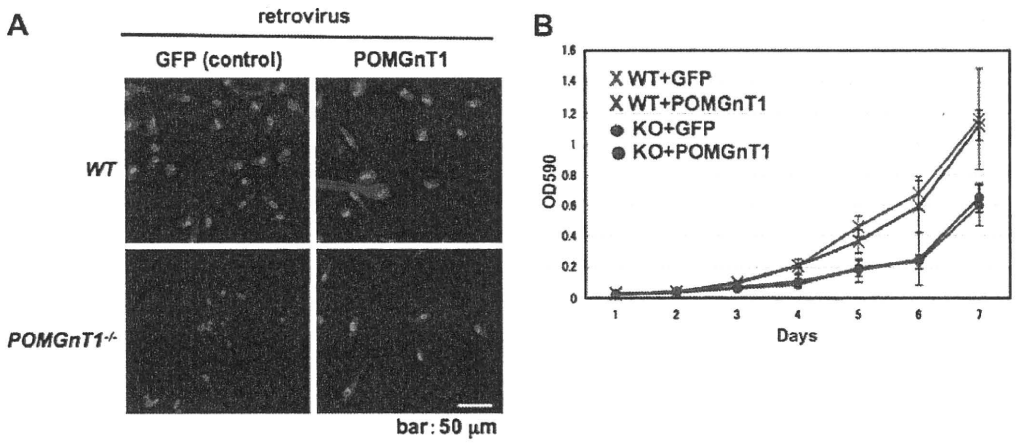

Fig. 8 – Restoration of POMGnT1 expression in *POMGnT1*$^{-/-}$ myoblasts does not improve proliferation of cells. (A) Wild-type (WT) and *POMGnT1*$^{-/-}$ myoblasts were transduced with a retrovirus expressing both POMGnT1 and GFP (POMGnT1) or only GFP (GFP, control), and the FACS-purified transduced cells were stained with anti-glycosylated α-DG monoclonal antibody (VIA4-1; red) and DAPI (Nucleus, blue). Note that the glycosylation of α-DG in *POMGnT1*$^{-/-}$ myoblasts was completely recovered by a retrovirus vector expressing POMGnT1. (B) MTT assay of wild-type (WT) and *POMGnT1*$^{-/-}$ myoblasts after infection with retrovirus vectors. Impaired proliferation of *POMGnT1*$^{-/-}$ myoblasts was not recovered by retrovirus-mediated expression of *POMGnT1*. Representative data of three independent experiments are shown.

3.2. *Null mutation in POMGnT1 reduces proliferative activity of muscle satellite cells*

POMGnT1$^{-/-}$ myoblasts proliferate poorly *in vitro*. This observation suggested that the proliferation of myoblasts is stimulated by growth signals *via* laminin-α-DG interaction. However, retrovirus vector-mediated gene transfer of the *POMGnT1* gene, which successfully restored O-mannosyl glycosylation of α-DG, did not restore the proliferation activity of the *POMGnT1*$^{-/-}$ myoblasts. DMD myoblasts proliferate poorly and quickly reach senescence. The impaired proliferation activity has been ascribed to repeated activation of

satellite cells due to repetitive cycles of muscle degeneration and regeneration (Blau et al., 1983). In contrast, POMGnT1$^{-/-}$ muscle lacks signs of active regeneration. Therefore, the reduced proliferation activity of POMGnT1$^{-/-}$ mouse myoblasts is not likely due to excessive cell division of satellite cells. Rather, it is likely that α-DG-laminin interaction in the niche, i.e. beneath the basal lamina of skeletal muscle myofibers, is important for maintenance of proliferative activity of satellite cells. However, the possibility that POMGnT1-deficiency causes aberrant glycosylation of molecules other than α-DG should be also tested.

Our results also suggested that the lack of α-DG-laminin interaction resulted in reduced numbers of muscle fibers (hypoplasia). Importantly, we found that myofibers of older POMGnT1$^{-/-}$ mice tend to be hypertrophied (Supplementary Fig. 2). POMGnT1$^{-/-}$ muscle might compensate the muscle power by hypertrophy of the myofibers. This is consistent with our observation that POMGnT1$^{-/-}$ muscle increases its mass in an overload model (unpublished data). Importantly, recent studies suggest that this process is satellite cell-independent (Sandri M., 2008).

Recently, Liu et al. showed that over-expression of integrin α7β1 in C2C12 myoblasts promoted proliferation of the cells (Liu et al., 2008). Importantly, however, we did not observe up-regulation of integrin α7β1 expression in POMGnT1$^{-/-}$ satellite cells. These observations suggest that dystroglycans and integrins have distinct roles in the regulation of muscle satellite cells.

In summary, we generated POMGnT1-null mice. The mice showed low serum creatine kinase levels and minimal signs of muscle degeneration and regeneration. Nonetheless, POMGnT1$^{-/-}$ muscle showed the reduction in the size and the number of myofibers. Furthermore, repeated injection of cardiotoxin showed impaired muscle regeneration in POMGnT1$^{-/-}$ mice. POMGnT1$^{-/-}$ myoblasts proliferated poorly *in vitro*. Over-expression of protein restored glycosylation of α-DG, but did not improve the proliferation of POMGnT1$^{-/-}$ myoblasts at all. Collectively, our results suggest that POMGnT1 enzymatic activity is important for maintenance of the proliferative activity of satellite cells *in vivo*.

4. Experimental procedures

4.1. Generation of POMGnT1$^{-/-}$ mice

The targeting strategy in ES cells is depicted in Fig. 1. Genomic DNA (8.6 kb) covering almost the entire POMGnT1 gene was isolated from 129/SvJ mice by using two specific primers: m1F2 primer, 5′-gat tcc tga agt cat gga ctg gc-3′ and m1B5, 5′-tct aaa ggt ctc tgt gtg agt ctg tca g-3′. The PCR product was then cloned into a TOPO TA cloning vector (Invitrogen, Carlsbad, CA) and sequenced (AB053221). To construct the targeting vector, a 630-bp RsrII-Hind III fragment, containing exon18 was replaced with a *neo* expression cassette (Stratagene) (Fig. 1). Electroporation and screening of ES cells (129Svev origin) were performed by Ingenious Targeting Laboratory, Inc. (Stony Brook, NY). Homologous recombination in ES cells was confirmed by Southern blotting. Two independent positive ES clones were injected into C57BL/6 blastocysts, which gave rise to offspring carrying the mutated allele. Genotyping of the mice was done by PCR. One primer set is designed to amplify exon 18: F2, 5′-cag cag ttt cct tcc ttc taa ccc-3′ and B4, 5′-att tgg tct ggt ccc ttg gct c-3′ (278 bp). *Neo* primers were used to amplify the *neo* resistance gene, and thereby detect the mutant allele: neo-F, 5′-agg cta ttc ggc tat gac tgg g-3′, and neo-R, 5′-tac ttt ctc ggc agg agc aag gtg-3′ (288 bp). Dystrophin-deficient *mdx* mice of C57BL/6 genetic background were provided by T. Sasaoka at the National Institute for Basic Biology, Japan. The Experimental Animal Care and Use Committee of the National Institute of Neuroscience approved all experimental protocols.

4.2. POMGnT1 enzymatic activity

Brains were obtained from 8-week-old mice and homogenized with nine volumes (weight/volume) of 10 mM Tris–HCl, pH 7.4, 1 mM EDTA, and 250 mM sucrose. After centrifugation at 900*g* for 10 min, the supernatant was subjected to ultracentrifugation at 100,000*g* for 1 h. The precipitates were used as the microsomal membrane fraction. The protein concentration was determined by BCA assay (Pierce, Rockford, IL). The enzymatic activity assay measured the amount of [^{3}H]GlcNAc transferred to a mannosyl peptide (Akasaka-Manya et al., 2004). Briefly, a reaction mixture containing 140 mM Mes buffer (pH 7.0), 1 mM UDP-[^{3}H]GlcNAc (80,000 dpm/nmol, PerkinElmer, Inc., Wellesley, MA), 2 mM mannosyl peptide (Ac-Ala-Ala-Pro-Thr-(Man)-Pro-Val-Ala-Ala-Pro-NH_2), 10 mM $MnCl_2$, 2% Triton X-100, 5 mM AMP, 200 mM GlcNAc, 10% glycerol, and 100 μg of microsomal membrane fraction was incubated at 37 °C for 1 h. After boiling for 3 min, the mixture was analyzed by reverse phase HPLC using a Wakopak 5C18-200 column (4.6 × 250 mm, Wako Pure Chemical Industries, Osaka, Japan). The gradient solvents were aqueous 0.1% trifluoroacetic acid (solvent A) and acetonitrile containing 0.1% trifluoroacetic acid (solvent B). The mobile phase consisted of 100% A for 10 min and then a linear gradient to 75% A:25% B over 25 min. Peptide separation was monitored at 214 nm, and the radioactivity of each fraction (1 ml) was measured using a liquid scintillation counter.

4.3. Antibodies

All antibodies used in Western blotting, immunohistochemistry, and FACS are listed in Supplementary Table 1.

4.4. Histology and immunohistochemical analysis

Muscle cryosections (6–10 μm) were stained with hematoxylin and eosin (H&E), or treated with 0.1% Triton X-100, blocked with 5% goat serum/1% BSA in PBS, then incubated with primary antibodies (Supplementary Table 1) at 4 °C overnight. After washing with PBS, specimens were incubated with a secondary antibody labeled with Alexa Fluor 488 or Alexa Fluor 568 (1:200–400 dilution; Molecular Probes) at RT for 1 h, counterstained with TOTO-3 (1:5000; Molecular Probes), and then mounted in Vectashield (Vector). The images were recorded using a confocal laser scanning microscope system TCSSP™ (Leica). For fiber size measurement, cross-sections of muscle were stained with anti-laminin α2

antibody and recorded and quantified by a digital microscope, BIOREVO (http://www.biorevo.jp; KEYENCE, Osaka, Japan).

4.5. Western blotting

Western blotting was performed as previously described (Hosaka et al., 2002). In brief, 20 μg of muscle proteins were separated on 7.5% SDS–PAGE gels and transferred to a PVDF membrane (Millipore, Bedford, MA). After incubation with primary antibodies (Supplementary Table 1), the membranes were incubated in HRP-labeled secondary antibodies (1:5000 dilution) (Amersham Biosciences, UK). The signals were detected by using an ECL plus Western Blotting Detection System (GE Healthcare, Buckinghamshire, UK).

4.6. Laminin blot overlay assay

An overlay assay was performed as described by Moore et al. (2002). In brief, WGA-enriched homogenates were prepared from wild-type and *POMGnT1*$^{-/-}$ brains, separated on SDS–PAGE gels, blotted onto a PDVF membrane, and incubated with mouse EHS laminin (Trevigen, Gaithersburg, MD, USA). Bound laminin was probed with anti-laminin antibody (Sigma, St. Louis, MO) and ECL system (GE Healthcare, Buckinghamshire, UK).

4.7. Single fiber preparation and culture

Single fibers were prepared from extensor digitorum longus (EDL) and soleus muscles of wild-type and *POMGnT1*$^{-/-}$ mice as described by Rosenblatt et al. (1995). Each fiber was plated onto Matrigel (BD Biosciences, Bedford, MA)-coated 24-well plates and cultured in growth medium for 3 days. Then, the number of cells around the parental fiber was counted.

4.8. Isolation of satellite cells, proliferation assay, and fusion index

Satellite cells were prepared from wild-type and *POMGnT1*$^{-/-}$ mice by FACS as previously described (Fukada et al., 2007). Sorted cells were plated on Matrigel-coated 24-well-plates at a density of 1×10^4 cells/well in a growth medium, DMEM (High glucose; Wako, Osaka), supplemented with 20% fetal bovine serum (Equitech-bio, Inc., Kerville, TX), human recombinant bFGF (2.5 ng/ml) (Invitrogen), recombinant mouse HGF (25 ng/ml) (R&D Systems, Minneapolis, MN), and heparin (5 μg/ml) (Sigma). For the MTT assay, 100 μl of 0.5% MTT (3-(4,5-dimethylthiazol-2-yl)-2,5-diphenyltetrazolium bromide) (Dojindo, Kumamoto, Japan) was added to the culture at each time point, and after 4 h incubation, the cells were collected in 1 ml of acid isopropanol solution. OD_{590} was measured and plotted. After reaching 70% confluency, the cells were induced to differentiate into myotubes by low-serum medium (5% horse serum/DMEM), and 18 h later, the cells were fixed, stained with anti-sarcomeric α-actinin antibody and DAPI (nuclei). Fusion index was calculated as (the numbers of nuclei in the myotubes/total nuclei) × 100%.

4.9. Production of retrovirus vectors

pMXs-IG (Kitamura et al., 2003) was kindly provided by T.Kitamura at Tokyo University. Human POMGnT1 cDNA, which has an Xpress epitope and a His-tag at the N-terminal (Akasaka-Manya et al., 2004), was cloned into the multi-cloning site upstream of IRES-GFP of the vector. Vector particles were produced by transfection of the vector plasmid into PLAT-E packaging cells (Kitamura et al., 2003). Proliferating satellite cells (myoblasts) were incubated with the viral vectors overnight and 4 days later, successfully transduced GFP-positive cells were collected by FACS, and the proliferation rate was evaluated by MTT assay.

4.10. Electron microscopy

Mice were perfused transcardially with a solution of 2% paraformaldehyde and 2.5% glutaraldehyde in PBS under deep pentobarbital anesthesia. The anterior tibial muscles were excised, embedded in 3% agarose, and sections (70 μm in thickness) were prepared on a Vibratome. Sections were fixed in OsO_4, ehydrated, and embedded in Cartepoxy resin. Ultrathin sections were prepared, stained with lead citrate and uranyl acetate, and observed under a Hitachi H-7000 transmission electron microscope.

4.11. Measurement of serum creatine kinase (CK)

Blood samples were obtained from the tail vein or directly from the heart at sacrifice. Serum CK level was measured by colorimetric assay using an FDC3500 clinical biochemistry autoanalyzer (FujiFilm Medical Co., Tokyo, Japan).

4.12. Cardiotoxin (CTX) injection

To induce muscle regeneration, CTX (10 μmol/L in saline; Sigma, St. Louis, MO) was injected into the tibialis anterior (TA) muscles three times at indicated intervals. The muscle cross-sections were stained with Oil red O (Muto Pure Chemicals Co., Ltd., Tokyo, Japan) to detect lipid droplets, or with Sirius red F3B (Sigma Chemical Co., St. Louis, MO) in saturated picric acid to stain collagen fibers.

Acknowledgments

This work was supported by Health Science Research Grants for Research on the Human Genome and Gene Therapy (H16-genome-003). For research on Phychiatric and Neurological Diseases and Mental Health (H18-kokoro-019; H20-016) from the Japanese Ministry of Health, Labor and Welfare, and Grants-in-Aid for Scientific Research (18590392) from the Japanese Ministry of Education, Culture, Sports, Science and Technology.

Appendix A. Supplementary data

Supplementary data associated with this article can be found, in the online version, at doi:10.1016/j.mod.2008.12.001.

REFERENCES

Akasaka-Manya, K., Manya, H., Kobayashi, K., Toda, T., Endo, T., 2004. Structure–function analysis of human protein O-linked mannose beta1,2-N-acetylglucosaminyltransferase 1, POMGnT1. Biochem. Biophys. Res. Commun. 320, 39–44.

Blau, H.M., Webster, C., Pavlath, G.K., 1983. Defective myoblasts identified in Duchenne muscular dystrophy. Proc. Natl. Acad. Sci. USA 80, 4856–4860.

Burkin, D.J., Wallace, G.Q., Milner, D.J., Chaney, E.J., Mulligan, J.A., Kaufman, S.J., 2005. Transgenic expression of α7β1 integrin maintains muscle integrity, increases regenerative capacity, promotes hypertrophy, and reduces cardiomyopathy in dystrophic mice. Am. J. Pathol. 166, 253–263.

Burkin, D.J., Wallace, G.Q., Nicol, K.J., Kaufman, D.J., Kaufman, S.J., 2001. Enhanced expression of the alpha 7 beta 1 integrin reduces muscular dystrophy and restores viability in dystrophic mice. J. Cell Biol. 152, 1207–1218.

Campanelli, J.T., Roberds, S.L., Campbell, K.P., Scheller, R.H., 1994. A role for dystrophin-associated glycoproteins and utrophin in agrin-induced AChR clustering. Cell 77, 663–674.

Cohn, R.D., Henry, M.D., Michele, D.E., Barresi, R., Saito, F., Moore, S.A., Flanagan, J.D., Skwarchuk, M.W., Robbins, M.E., Mendell, J.R., Williamson, R.A., Campbell, K.P., 2002. Disruption of DAG1 in differentiated skeletal muscle reveals a role for dystroglycan in muscle regeneration. Cell 110, 639–648.

Endo, T., Toda, T., 2003. Glycosylation in congenital muscular dystrophies. Biol. Pharm. Bull. 26, 1641–1647.

Fukada, S., Uezumi, A., Ikemoto, M., Masuda, S., Segawa, M., Tanimura, N., Yamamoto, H., Miyagoe-Suzuki, Y., Takeda, S., 2007. Molecular signature of quiescent satellite cells in adult skeletal muscle. Stem Cells 25, 2448–2459.

Gee, S.H., Montanaro, F., Lindenbaum, M.H., Carbonetto, S., 1994. Dystroglycan-alpha, a dystrophin-associated glycoprotein, is a functional agrin receptor. Cell 77, 675–686.

Hosaka, Y., Yokota, T., Miyagoe-Suzuki, Y., Yuasa, K., Imamura, M., Matsuda, R., Ikemoto, T., Kameya, S., Takeda, S., 2002. Alpha1-syntrophin-deficient skeletal muscle exhibits hypertrophy and aberrant formation of neuromuscular junctions during regeneration. J. Cell Biol. 158, 1097–1107.

Hu, H., Yang, Y., Eade, A., Xiong, Y., Qi, Y., 2007. Breaches of the pial basement membrane and disappearance of the glia limitans during development underlie the cortical lamination defect in the mouse model of muscle-eye-brain disease. J. Comp. Neurol. 502, 168–183.

Ibraghimov-Beskrovnaya, O., Ervasti, J.M., Leveille, C.J., Slaughter, C.A., Sernett, S.W., Campbell, K.P., 1992. Primary structure of dystrophin-associated glycoproteins linking dystrophin to the extracellular matrix. Nature 355, 696–702.

Kanagawa, M., Michele, D.E., Satz, J.S., Barresi, R., Kusano, H., Sasaki, T., Timpl, R., Henry, M.D., Campbell, K.P., 2005. Disruption of perlecan binding and matrix assembly by post-translational or genetic disruption of dystroglycan function. FEBS Lett. 579, 4792–4796.

Kanagawa, M., Toda, T., 2006. The genetic and molecular basis of muscular dystrophy: roles of cell-matrix linkage in the pathogenesis. J. Hum. Genet. 51, 915–926.

Kitamura, T., Koshino, Y., Shibata, F., Oki, T., Nakajima, H., Nosaka, T., Kumagai, H., 2003. Retrovirus-mediated gene transfer and expression cloning: powerful tools in functional genomics. Exp. Hematol. 31, 1007–1014.

Liu, J., Ball, S.L., Yang, Y., Mei, P., Zhang, L., Shi, H., Kaminski, H.J., Lemmon, V.P., Hu, H., 2006. A genetic model for muscle-eye-brain disease in mice lacking protein O-mannose 1,2-N-acetylglucosaminyltransferase (POMGnT1). Mech. Dev. 123, 228–240.

Liu, J., Burkin, D.J., Kaufman, S.J., 2008. Increasing alpha 7 beta 1-integrin promotes muscle cell proliferation, adhesion, and resistance to apoptosis without changing gene expression. Am. J. Physiol. Cell Physiol. 294, C627–C640.

Michele, D.E., Barresi, R., Kanagawa, M., Saito, F., Cohn, R.D., Satz, J.S., Dollar, J., Nishino, I., Kelley, R.I., Somer, H., Straub, V., Mathews, K.D., Moore, S.A., Campbell, K.P., 2002. Post-translational disruption of dystroglycan–ligand interactions in congenital muscular dystrophies. Nature 418, 417–422.

Moore, S.A., Saito, F., Chen, J., Michele, D.E., Henry, M.D., Messing, A., Cohn, R.D., Ross-Barta, S.E., Westra, S., Williamson, R.A., Hoshi, T., Campbell, K.P., 2002. Deletion of brain dystroglycan recapitulates aspects of congenital muscular dystrophy. Nature 418, 422–425.

Peng, H.B., Ali, A.A., Daggett, D.F., Rauvala, H., Hassell, J.R., Smalheiser, N.R., 1998. The relationship between perlecan and dystroglycan and its implication in the formation of the neuromuscular junction. Cell Adhes. Commun. 5, 475–89.

Rosenblatt, J.D., Lunt, A.I., Parry, D.J., Partridge, T.A., 1995. Culturing satellite cells from living single muscle fiber explants. In Vitro Cell Dev. Biol. Anim. 31, 773–779.

Sandri M., 2008. Signaling in muscle atrophy and hypertrophy. Physiology (Bethesda) 23, 160–170.

Sugita, S., Saito, F., Tang, J., Satz, J., Campbell, K., Südhof, T.C., 2001. A stoichiometric complex of neurexins and dystroglycan in brain. J. Cell Biol. 154, 435–445.

Voit, T., Tome, F.S., 2004. The congenital muscular dystrophies. In: Engel, A.G., Franzini-Armstrong, C. (Eds.), Myology. McGraw-Hill, New York, pp. 1203–1238.

Yang, Y., Zhang, P., Xiong, Y., Li, X., Qi, Y., Hu, H., 2007. Ectopia of meningeal fibroblasts and reactive gliosis in the cerebral cortex of the mouse model of muscle-eye-brain disease. J. Comp. Neurol. 505, 459–477.

Yoshida, A., Kobayashi, K., Manya, H., Taniguchi, K., Kano, H., Mizuno, M., Inazu, T., Mitsuhashi, H., Takahashi, S., Takeuchi, M., Herrmann, R., Straub, V., Talim, B., Voit, T., Topaloglu, H., Toda, T., Endo, T., 2001. Muscular dystrophy and neuronal migration disorder caused by mutations in a glycosyltransferase, POMGnT1. Dev. Cell 1, 717–724.

Cell Metabolism

Crosstalk between Glucocorticoid Receptor and Nutritional Sensor mTOR in Skeletal Muscle

Noriaki Shimizu,[1,10] Noritada Yoshikawa,[1,2,10] Naoki Ito,[3,4] Takako Maruyama,[1] Yuko Suzuki,[3] Sin-ichi Takeda,[3] Jun Nakae,[5] Yusuke Tagata,[9] Shinobu Nishitani,[9] Kenji Takehana,[9] Motoaki Sano,[6] Keiichi Fukuda,[6] Makoto Suematsu,[7,8] Chikao Morimoto,[1,2] and Hirotoshi Tanaka[1,2,*]

[1]Division of Clinical Immunology, Advanced Clinical Research Center
[2]Department of Rheumatology and Allergy, Research Hospital
Institute of Medical Science, University of Tokyo, Tokyo 108-8639, Japan
[3]Department of Molecular Therapy, National Institute of Neuroscience, National Center of Neurology and Psychiatry, Kodaira 187-8502, Japan
[4]Department of Biological Information, Tokyo Institute of Technology, Yokohama 226-8501, Japan
[5]Frontier Medicine on Metabolic Syndrome, Division of Endocrinology, Metabolism and Nephrology, Department of Internal Medicine
[6]Cardiology Division, Department of Internal Medicine
[7]Department of Biochemistry
[8]JST ERATO, Suematsu Gas Biology Project
Keio University School of Medicine, Tokyo 160-8582, Japan
[9]Ajinomoto Pharmaceuticals Co., Ltd., Kawasaki 210-8681, Japan
[10]These authors contributed equally to this work
*Correspondence: hirotnk@ims.u-tokyo.ac.jp
DOI 10.1016/j.cmet.2011.01.001

SUMMARY

Maintenance of skeletal muscle mass relies on the dynamic balance between anabolic and catabolic processes and is important for motility, systemic energy homeostasis, and viability. We identified direct target genes of the glucocorticoid receptor (GR) in skeletal muscle, i.e., REDD1 and KLF15. As well as REDD1, KLF15 inhibits mTOR activity, but via a distinct mechanism involving BCAT2 gene activation. Moreover, KLF15 upregulates the expression of the E3 ubiquitin ligases atrogin-1 and MuRF1 genes and negatively modulates myofiber size. Thus, GR is a liaison involving a variety of downstream molecular cascades toward muscle atrophy. Notably, mTOR activation inhibits GR transcription function and efficiently counteracts the catabolic processes provoked by glucocorticoids. This mutually exclusive crosstalk between GR and mTOR, a highly coordinated interaction between the catabolic hormone signal and the anabolic machinery, may be a rational mechanism for fine-tuning of muscle volume and a potential therapeutic target for muscle wasting.

INTRODUCTION

Muscle comprises ~40% of body mass and contributes not only to the structure and movement of the body but also to nutrient storage and supply (Matthews, 1999). In adult mammals, skeletal muscle hypertrophy/atrophy is characterized by an increase/decrease in the size (as opposed to the number) of individual myofibers, respectively. The control of muscle mass is believed to be determined by a dynamic balance between anabolic and catabolic processes (Hoffman and Nader, 2004). Mammalian target of rapamycin (mTOR) is a crucial component of the anabolic machinery for protein synthesis. mTOR consists of two complexes: mTORC1, which includes Raptor, signals to S6K and 4E-BP1, controls protein synthesis, and is rapamycin sensitive; and mTORC2, which includes Rictor, signals to Akt, and is rapamycin insensitive. mTORC1 integrates four major signals: growth factors, energy status, oxygen, and amino acids, especially branched-chain amino acids (BCAAs). Prototypically, insulin/IGF-1 activates mTOR via the PI3K-Akt pathway (Sengupta et al., 2010). It is currently considered that mTORC1, and not mTORC2, is essential for the maintenance of muscle mass and function (Bentzinger et al., 2008; Risson et al., 2009). Protein degradation in skeletal muscle cells is essentially mediated by the activity of two conserved pathways: the ubiquitin-proteasomal pathway and the autophagic/lysosomal pathway (Sandri, 2008). The ubiquitin-proteasomal pathway is responsible for the turnover of the majority of soluble and myofibrillar muscle proteins. The activity of this pathway is markedly increased in atrophying muscle due to the transcriptional activation of a set of E3 ligase-encoding genes, e.g., atrogin-1 and MuRF1 (Glass, 2003; Sandri et al., 2004). Autophagy also plays an important role in the degradation of skeletal muscle, and is indicated to be a consequence of an ordered transcriptional program involving a battery of genes, e.g., LC3 and Bnip3 (Mizushima et al., 2008). These positive and negative pathways are balanced in a highly coordinated manner for the determination of myofiber size and total muscle volume; however, distortion of this balance with a relative increase in degradation results in the generalized decrease of myofiber size and muscle atrophy (Hoffman and Nader, 2004). Pioneering studies demonstrated that muscle atrophy is a result of active processes that are transcriptionally controlled through the expression of a particular gene set; the forkhead box O (FoxO) transcription factors are

common components of a number of atrophy models and act as critical liaison molecules for protein degradation and autophagy via the transcriptional regulation of, for example, atrogin-1, MuRF1, LC3, and Bnip3 (Mammucari et al., 2007; Sandri et al., 2004; Stitt et al., 2004; Zhao et al., 2007). In clear contrast, it is evident that each disease has proper signaling pathways to FoxOs and that other components of the cellular machinery often participate in the progression of atrophy (Moresi et al., 2010; Suzuki et al., 2007). Therefore, for the development of therapies against muscle atrophy, it should be addressed how the transcriptional program triggered by a particular atrophy pathway is orchestrated and how the balance of muscle protein synthesis and degradation is distorted in each disease.

Adrenal glucocorticoids produce their actions via a signal pathway involving the ubiquitously expressed glucocorticoid receptor (GR), a prototypic member of the nuclear receptor superfamily, which acts as a ligand-dependent transcription factor. Upon binding glucocorticoids, GR translocates into the nucleus and binds to the glucocorticoid response element (GRE) in the promoters of target genes. The binding of liganded receptors to target DNA is followed by the recruitment of mediators and coactivators to the proximity of GRE, resulting in the recruitment of RNA polymerase II (RNAPII) to nearby transcription start sites and the activation of transcription (Evans, 2005; Meijsing et al., 2009). In skeletal muscle, glucocorticoids elicit a variety of biological actions in the metabolism of glucose, lipids, and proteins and contribute to metabolic homeostasis (Munck et al., 1984). On the other hand, the prolonged oversecretion or exogenous administration of glucocorticoid gives rise to undesirable effects including muscle atrophy (Munck et al., 1984). Although many studies addressed the mechanism of glucocorticoid-induced muscle atrophy, how the glucocorticoid-GR system generates the functional coupling between metabolic regulation and volume adjustment in skeletal muscle remains unsolved. Of note, many pathological conditions characterized by muscle atrophy, e.g., sepsis, cachexia, starvation, metabolic acidosis, and severe insulinopenia, are associated with an increase in circulating glucocorticoid levels. Adrenalectomy or treatment with the GR antagonist RU486 attenuates muscle atrophy in sepsis, cachexia, starvation, and severe insulinopenia (Menconi et al., 2007; Schakman et al., 2008). Moreover, endogenous glucocorticoids were shown to be essential for muscle atrophy in acute diabetic rodents (Hu et al., 2009). Together, understanding the glucocorticoid-mediated regulation of metabolism-volume coupling in muscle is increasingly important for the management of not only muscle atrophy but also these wasting/metabolic disorders.

Typically, glucocorticoid-induced muscle atrophy is characterized by fast-twitch type II glycolytic muscle fiber loss with reduced or no impact on type I fibers. The mechanism of such fiber specificity is yet unknown. Previous reports suggested that the glucocorticoid-GR system has antianabolic and catabolic effects and promotes degradation via the induction of a set of genes including atrogin-1, MuRF1, and myostatin (Menconi et al., 2007; Schakman et al., 2008). Although the involvement of FoxO transcription factors is reported in the gene regulation of atrogin-1 and MuRF1 under the presence of excess glucocorticoids (Sandri et al., 2004; Stitt et al., 2004), the biochemical role of GR in the transcriptional regulation of muscle tissue has not yet been determined. Therefore, we investigated how GR-mediated gene expression coordinately modulates antianabolic and catabolic actions to understand the functional coupling of metabolism and volume regulation in muscle.

In the present study, we identified REDD1 and KLF15 genes as direct targets of GR. REDD1 is known to be induced by various stressors, including glucocorticoid, and to inhibit mTOR activity via the sequestration of 14-3-3 and the increase of TSC1/2 activity (Wang et al., 2006; DeYoung et al., 2008). We clearly identified the functional GRE via the promoter analysis of REDD1 gene. On the other hand, KLF15 is a recently discovered transcription factor that is involved in several metabolic processes in skeletal muscle; e.g., KLF15 transcriptionally upregulates the gene expression of branched-chain aminotransferase 2 (BCAT2), a mitochondrial enzyme catalyzing the first reaction in the catabolism of BCAA to accelerate BCAA degradation and alanine production in skeletal muscle (Gray et al., 2007). Moreover, phenotypic analysis of cardiac-specific KLF15 knockout mice revealed marked left ventricular hypertrophy, indicating the negative regulatory role of KLF15 on muscle mass (Fisch et al., 2007). We here demonstrated that KLF15 participates in muscle catabolism via the transcriptional regulation of atrogin-1 and MuRF1. Moreover, KLF15 affects mTOR through BCAA degradation and negatively modulates myofiber size. mTOR activation inhibits GR-mediated transcription by suppressing GR recruitment onto target genes, strongly suggesting a mutually exclusive crosstalk between mTOR and GR. Pharmacological activation of mTOR with BCAA attenuated GR-mediated gene expression, leading to the substantial restoration of muscle in glucocorticoid-treated rats. We, therefore, indicate the critical importance of the interaction of GR and mTOR in the regulation of metabolism-volume coupling in skeletal muscle.

RESULTS

REDD1 and KLF15 Are Target Genes of GR in Skeletal Muscle

GR levels were relatively high in type II-rich gastrocnemius and tibialis anterior muscles compared to type I-rich soleus muscle in rats (Figure 1A). Figure 1B illustrates the comparison of the effects of a 3 hr treatment with dexamethasone (DEX) on mRNA expression of various genes between the gastrocnemius and soleus muscles. Hormonal induction of mRNA expression of REDD1, atrogin-1, MuRF1, KLF15, FoxO1, FoxO3, and myostatin, as well as the well-known GR target gene FKBP5 (Yoshikawa et al., 2009), was observed in both muscles, but to a lesser extent in the soleus muscle. Among the genes induced by DEX at 3 hr (Figure 1B), the promoter regions of MuRF1 (Waddell et al., 2008) and myostatin (Ma et al., 2001), but not atrogin-1 (Sandri et al., 2004), contain functional GREs. In addition, REDD1 and KLF15 were also considered as candidates of GR target genes (see the Supplemental Information available online).

Concerning KLF15, we showed, in gastrocnemius muscle and L6 myotubes but not in liver, that KLF15 mRNA and protein expression was induced in a GR-dependent manner (Figure 2A). The promoter region spanning from −4676 to +116 of KLF15 gene was not responsive to DEX; however, the activity of the region spanning −2108 to +1331 was induced by DEX, and

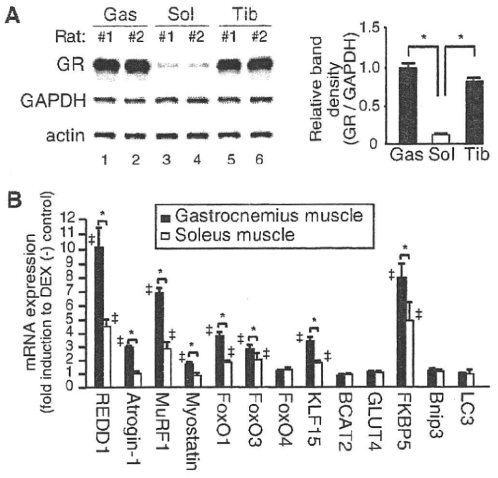

Figure 1. GR Protein Expression and Glucocorticoid-Dependent mRNA Expression of Atrophy-Related Genes in Rat Skeletal Muscles

(A) GR protein levels in rat gastrocnemius (Gas), soleus (Sol), and tibialis anterior (Tib). Left, representative immunoblots. Right, quantified protein levels of GR relative to GAPDH (n = 9).

(B) Induction of mRNA levels of atrophy-related genes by dexamethasone (DEX). Expression levels of the indicated mRNA in the muscles from rats 3 hr after intraperitoneal injection with DEX were assessed in quantitative RT-PCR (qRT-PCR). Results are shown as fold induction to vehicle-treated rats (n = 6).

(A and B) Error bars show SD. $^{*}p < 0.05$, $^{\ddagger}p < 0.05$ versus vehicle-treated rats.

this induction was inhibited by a GR antagonist RU486. The deletion and mutational analyses of KLF15 promoter indicated that both upper GRE1 and lower GRE2 sites were functional (Figures 2B and 2C). The transient transfection assays using the reporter constructs conveying these minimal GRE sites clearly showed that each GRE is independently functional (Figure 2D). A chromatin immunoprecipitation (ChIP) assay revealed that both GRE-like sequences were targeted by GR and that RNAPII was incorporated onto the coding region of KLF15 gene in the presence of DEX in L6 cells (Figure 2E). We also confirmed the DEX-dependent recruitment of endogenous GR onto the KLF15 promoter in a skeletal muscle-specific manner in vivo (Figure 2F). Similarly, we identified the functional GRE on the REDD1 promoter region and confirmed REDD1 as a GR target gene as well (Figure S1).

KLF15 Transactivates atrogin-1 and MuRF1 Genes

Next, we studied the alteration in the gene expression profile after the direct injection of a KLF15-expressing adenovirus into the rat tibialis anterior muscle. The exogenous expression of KLF15 increased KLF15 protein levels by approximately 5-fold (Figure 3A) and significantly induced mRNA expression of its target gene BCAT2 as anticipated (Figure 3B). Moreover, mRNA expression of atrogin-1, MuRF1, FoxO1, and FoxO3 was stimulated by KLF15 (Figure 3B). We then focused on atrogin-1 and MuRF1 and asked whether the DEX-mediated induction of their mRNA expression was dependent on KLF15. For that purpose, we tested the effect of knocking down the expression of GR or KLF15 on mRNA expression of KLF15, atrogin-1, and MuRF1 as well as another GR target gene REDD1 as a control. In L6 myoblasts, GR knockdown diminished the DEX-dependent mRNA induction of all of these GR target genes. However, KLF15 knockdown affected that of atrogin-1 and MuRF1 but not REDD1 (Figure 3C). These results strongly indicate the critical involvement of the GR-KLF15 cascade in the DEX-mediated upregulation of atrogin-1 and MuRF1 gene expression. To address the role of KLF15 in the transcriptional regulation of atrogin-1 and MuRF1, we constructed luciferase reporter plasmids driven by the promoter of rat atrogin-1 or MuRF1, and tested the effect of the exogenous expression of KLF15 in L6 myoblasts. The expression of the reporter genes was upregulated in a KLF15-dependent manner (Figure 3D). Since the promoter regions of atrogin-1 and MuRF1 contain a number of putative KLF15 recognition sites, we performed ChIP analyses; both promoters had multiple KLF15 binding sites and some of them were located in the proximity of FoxO binding sites and GRE (Figure 3E), and at least one of these KLF15 sites of each promoter recruited KLF15 in a DEX-dependent manner in vivo as well (Figure 3F). Note that atrogin-1 and MuRF1 were originally identified as FoxO target genes (Sandri et al., 2004; Waddell et al., 2008) and that KLF15 induced FoxO mRNA expression (Figure 3B). Indeed, the combination of KLF15 and FoxO significantly enhanced the promoter activity of atrogin-1 and MuRF1 when compared to their individual effects (Figure 3G). Moreover, the direct injection of the adenovirus expressing constitutively active FoxO1 or KLF15 significantly increased atrogin-1 and MuRF1 mRNA expression, and the expression of both resulted in synergistic or additive effects in tibialis anterior (Figure 3H). Therefore, it is likely that KLF15 and FoxO transcription factors cooperatively upregulate the expression of atrogin-1 and MuRF1 genes.

GR-KLF15 Axis Modulates BCAA Metabolism and mTOR Activity

Next, we studied the effects of glucocorticoids, GR, and KLF15 on BCAT2 and BCAA catabolism in skeletal muscle cells. In gastrocnemius muscle, mRNA expression of KLF15 preceded that of BCAT2 after treatment with DEX (Figure 4A). Overexpression of KLF15 increased the BCAT2 promoter-luciferase reporter activity (Figure 4B). Moreover, DEX-induced BCAT2 promoter activation was inhibited by either RU486 or siKLF15 (Figure 4C), indicating that KLF15 is mandatory for GR-mediated BCAT2 gene activation. BCAT2 enzyme activity was stimulated by DEX, and this effect was abolished in the presence of RU486 (Figure 4D). In tibialis anterior muscle and L6 myotubes, the adenovirus-mediated exogenous expression of KLF15 significantly induced BCAT2 enzyme activity even in the absence of DEX (Figure 4E).

The measurement of intracellular amino acid levels clearly revealed the accelerated catabolism of BCAA by KLF15 in myotubes; the exogenous expression of KLF15 decreased the levels of Val, Leu, and Ile, with a reciprocal increase in Ala and Glu without significant alterations in, for example, Gly, Trp, Gln, Tyr, and Phe, in L6 myotubes (Figure 4F). Amino acids, especially BCAA, are believed to activate mTOR and to increase in association with Rheb-mTOR (Sancak et al., 2010). We showed that overexpression of KLF15 in C2C12 myotubes suppressed mTOR activity as demonstrated by the decrease in the phosphorylated form of S6K1. Moreover, mTOR activity was complemented by the addition of excess BCAA (Figure 4G). Of note,

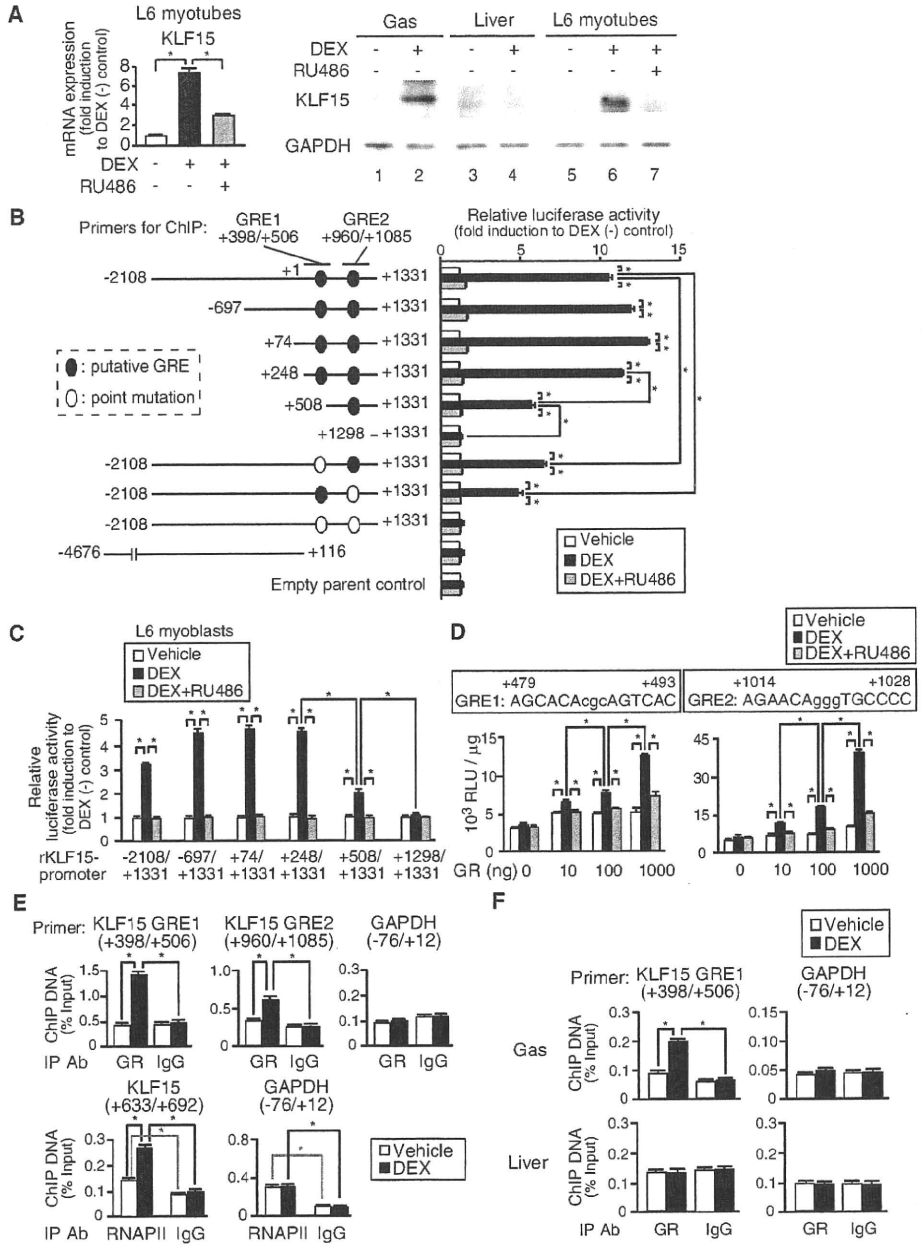

Figure 2. Identification of KLF15 as a Direct GR Target Gene

(A) GR-dependent mRNA (left) and protein (right) expression of KLF15 in L6 myotubes treated with DEX and RU486 for 6 hr and in DEX-treated rat gastrocnemius (see legend for Figure 1B).

(B) Identification of GREs in rat KLF15 promoter. Left, schematic of rat KLF15 promoter-luciferase reporter constructs. Positions of the primers for chromatin immunoprecipitation (ChIP) in (E) and (F) are shown. Right, GR-dependent activation of rat KLF15 promoter-reporter genes. COS-7 cells were transfected with the reporter constructs and 100 ng of GR expression plasmid and treated with DEX and RU486 for 18 hr.

(C) GR-dependent activation of rat KLF15 promoter-reporter genes in L6 myoblasts treated with DEX and RU486 for 18 hr.

(D) GR-dependent activation of reporter genes containing KLF15 promoter GREs. L6 myoblasts were transfected with the luciferase reporter constructs containing the GREs from rat KLF15 with GR expression plasmid and treated with DEX and RU486 for 18 hr.

(E) DEX-dependent recruitment of GR and RNAPII onto rat KLF15 gene. L6 myotubes treated with 1 µM DEX for 2 hr were subjected to ChIP.

(F) Skeletal muscle-specific recruitment of GR onto rat KLF15 gene by DEX. DEX-treated rat gastrocnemius (Gas) and liver (see legend for Figure 1B) were subjected to ChIP.

(A–F) Error bars show SD (n = 5). *$p < 0.05$.

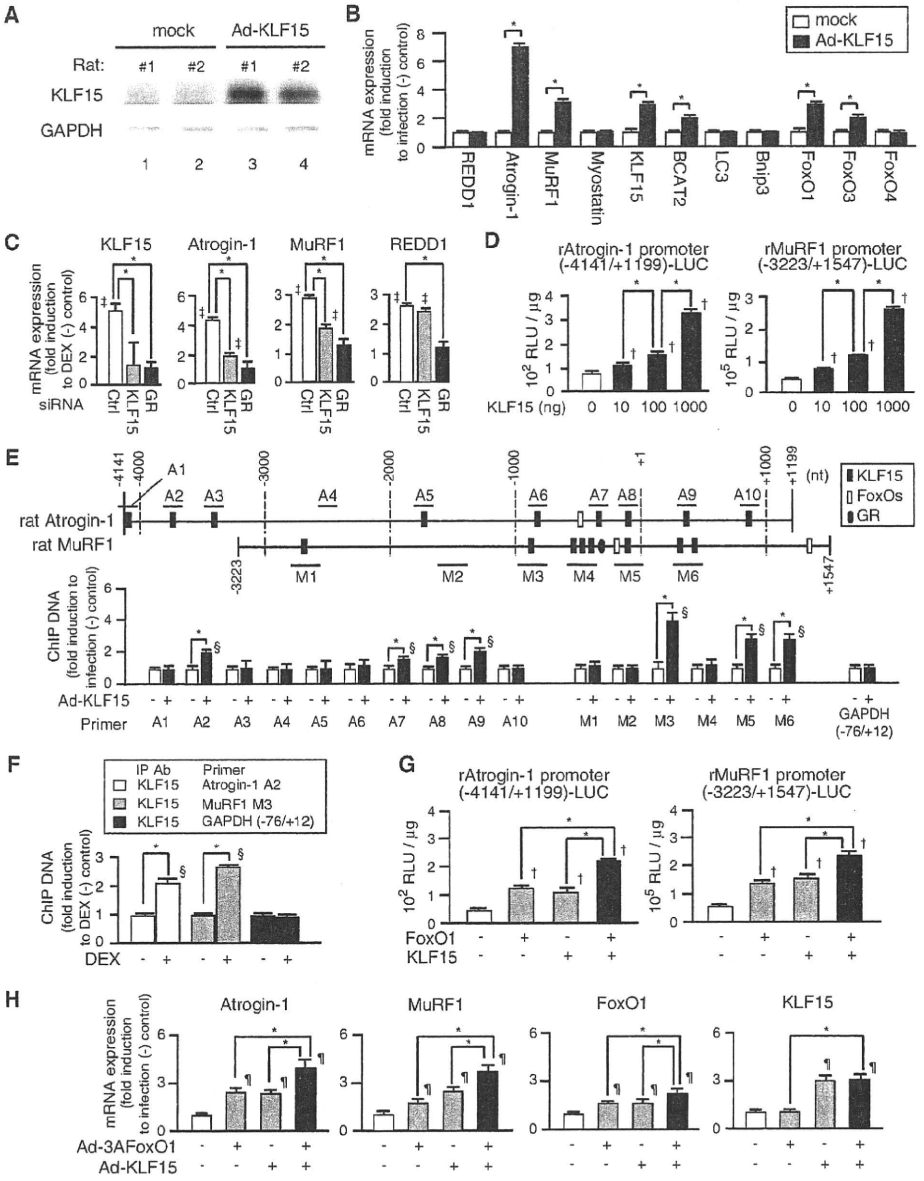

Figure 3. Transcriptional Regulation of Atrogenes by KLF15 and FoxOs

(A and B) KLF15-dependent mRNA expression of atrophy-related genes. Recombinant adenovirus Ad-KLF15 was infected to rat tibialis anterior for 7 days. (A) Immunoblot detection of ectopic KLF15. (B) qRT-PCR.

(C) Effects of knockdown of KLF15 or GR on DEX-dependent mRNA expression of atrophy-related genes. L6 myoblasts were transfected with control siRNA, siRNA against KLF15, or siRNA against GR and treated with DEX for 18 hr.

(D) KLF15-dependent activation of rat atrogin-1 (left) and MuRF1 (right) promoter-reporter genes in L6 myoblasts.

(E) Mapping of the binding sites for KLF15, FoxOs, and GR in rat atrogin-1 and MuRF1 promoters. Top, putative binding sites identified in in silico promoter analysis (see the Experimental Procedures and the Supplemental Information). Bars indicate the positions of the primers for ChIP. Bottom, recruitment of KLF15 onto rat atrogin-1 and MuRF1 promoters. L6 myotubes were infected with Ad-KLF15 for 5 days and subjected to ChIP using anti-KLF15 antibody.

(F) DEX-dependent recruitment of KLF15 onto rat atrogin-1 and MuRF1 promoters in rat gastrocnemius (see Figure 1B).

(G and H) Effects of FoxOs and KLF15 on rat atrogin-1 and MuRF1 promoter-reporter gene expression in L6 myoblasts (G) and on atrogin-1 and MuRF1 mRNA expression in rat tibialis anterior (H). (G) Luciferase assay of L6 myoblasts transfected with the reporter constructs with or without FoxO1 and/or KLF15 expression plasmids. (H) qRT-PCR analysis of rat tibialis anterior expressing ectopic KLF15 and/or constitutive active FoxO1 (3AFoxO1) for 3 days.

(B–H) Error bars show SD (n = 5). *$p < 0.05$, ‡$p < 0.05$ versus vehicle-treated cells, †$p < 0.05$ versus mock-transfected cells, §$p < 0.05$ versus ChIP with normal IgG, ¶$p < 0.05$ versus mock-infected rats.

the diameter of C2C12 myotubes was shortened by KLF15 and rescued by BCAA (Figure 4G). Moreover, exogenous KLF15 reduced mTOR activity with fiber type-independent atrophy in the tibialis anterior muscle (Figure 4H). Taken together, these data indicate that KLF15 is a liaison molecule for GR in the induction of atrogenes and the acceleration of BCAA catabolism and mTOR repression to decrease myofiber size.

mTOR Affects GR-Mediated Transcriptional Regulation

Since little is known about how glucocorticoid-mediated catabolic signal transduction is shut off, we next examined the effects of mTOR blockade using rapamycin on GR-mediated gene expression in L6 myotubes. Surprisingly, rapamycin significantly enhanced the DEX-induced mRNA expression of a number of GR target genes, including REDD1, atrogin-1, MuRF1, KLF15, FoxOs, and FKBP5 (Figure 5A). These results strongly suggest that mTOR blockade selectively enhances mRNA expression of GR target genes, i.e., mTOR activation appears to have a negative impact on GR-mediated gene expression. To further address this negative modulation of GR function by mTOR, we performed transient transfection assays using GR-responsive KLF15 promoter-Luc and GRE-Luc reporter genes in L6 myoblasts. A constitutively active mutant of Rheb, RhebS16H, which autonomously activates mTOR, repressed DEX-mediated reporter gene activation, and rapamycin inhibited these negative effects of RhebS16H (Figure 5B). Moreover, a major endogenous mTOR activator IGF-1 slightly enhanced S6K1 phosphorylation and did not affect DEX-induced GRE-Luc expression when cultured in amino acid-rich media. In clear contrast, in amino acid-deprived media, DEX-dependent induction of GRE-Luc was approximately doubled, and IGF-1 strongly phosphorylated S6K1 and suppressed DEX-induced GRE-Luc expression (Figure 5C). These results indicated that, regardless of the upstream pathways for mTOR activation, endogenous GR activity is negatively controlled by mTOR in L6 myoblasts.

We then asked the underlying mechanisms for mTOR-mediated GR suppression. To test whether mTOR-mediated GR repression is via global protein synthesis downstream of mTOR, we examined luciferase mRNA expression in transient transfection assay using GRE-Luc reporter plasmid in the presence or absence of the protein synthesis inhibitor cycloheximide. Cycloheximide did not influence on either GR-mediated GRE activation or BCAA-mediated GR suppression (Figure 5D). Therefore, BCAA inhibits the transcriptional effects of GR via mTOR activation but not via de novo protein synthesis. Immunoblotting using L6 myotubes revealed that GR protein levels were unaltered in the presence of DEX, BCAA, or rapamycin. Treatment with DEX clearly promoted the nuclear translocation of GR, and such a process was not affected by BCAA or rapamycin (Figure 5E). Concerning the promoter regions spanning the putative GREs in KLF15 and REDD1, DEX-induced GR recruitment was significantly enhanced by rapamycin, suggesting that mTOR negatively influences the access of GR to these promoters. Such an enhancement of GR promoter binding by rapamycin was paralleled by RNAPII recruitment onto the coding regions of KLF15 and REDD1 (Figure 5F). Thus, cellular mTOR activity negatively modulates GR transcriptional function, most possibly by altering the intranuclear behavior of GR. We finally examined the effect of constitutive mTOR activation by studying the impact of adeno-associated virus-driven RhebS16H expression on S6K1 activity and the gene expression profile of the tibialis anterior muscle from DEX-treated rats. RhebS16H-injected muscle had elevated levels of S6K1 phosphorylation and significant decreases in the induction response to DEX of a number of glucocorticoid-inducible genes, including REDD1, atrogin-1, MuRF1, FoxOs, KLF15, and FKBP5, when compared to mock-injected muscle (Figures 5G and 5H).

mTOR Activation Attenuates Glucocorticoid-Induced Muscle Atrophy

It should be noted that numerous studies examined the effects of BCAA on mTOR activity in glucocorticoid-induced atrophy models with conflicting results, the reason for which might be variations in the protocols used in those in vivo studies (Menconi et al., 2007; Schakman et al., 2008). We showed that the bolus administration of a BCAA cocktail via a gastric tube just before the peritoneal injection of DEX (Supplemental Information) resulted in sufficient and reproducible mTOR activation in the gastrocnemius muscle; the phosphorylated form of S6K1 was increased at 30 min after BCAA administration and returned to the baseline level after 90–180 min, even in the presence of DEX (Figure 6A). We then tested the effects of DEX, BCAA, and rapamycin on the protein levels and phosphorylation status of mTOR and its downstream effectors S6K1 and 4E-BP1 as well as Akt, the upstream activator of mTOR, in the rat glucocorticoid-induced atrophy model (5 day intraperitoneal DEX administration, see the Supplemental Information). In GR-rich gastrocnemius muscle, treatment with DEX suppressed the phosphorylation of S6K1 and 4E-BP1, without a significant alteration in p-Akt, indicating that DEX inhibited mTOR function in an Akt-independent fashion in this model. In clear contrast, in either the soleus muscle or liver, DEX treatment did not affect mTOR activity. When BCAA was supplemented, the levels of p-S6K1 and p-4E-BP1 were efficiently restored. Of note, rapamycin canceled these effects of BCAA (Figure 6B). In this model, BCAA administration suppressed the glucocorticoid-induced expression of REDD1, atrogin-1, MuRF1, KLF15, FoxOs, and FKBP5 mRNA (Figure 6C), and there was a decrease in GR recruitment onto the promoters of KLF15, REDD1, MuRF1, and FKBP5 (Figure 6D). BCAA administration also repressed the expression of BCAT2, GLUT4, Bnip3, and LC3 mRNA, and treatment with rapamycin inhibited the effects of BCAA (Figure 6C). In contrast, in the soleus muscle, treatment with DEX alone or DEX plus BCAA only marginally influenced mTOR activity and the gene expression profile, if at all (Figures 6B and 6C).

In this glucocorticoid-induced muscle atrophy rat model, there was a decrease in the body weight of the DEX, DEX plus BCAA, and DEX plus BCAA plus rapamycin groups (Figure 7A). The DEX plus BCAA group revealed a significant restoration of muscle strength as determined by a grip test and the weight of the gastrocnemius muscle when compared with DEX group (Figures 7B and 7C). Histological examination of the gastrocnemius muscle demonstrated typical type II fiber-dominant atrophy in the DEX group; however, the DEX plus BCAA group showed less impairment in the gastrocnemius muscle that was represented by the prevention of type II fiber loss. Semiquantitative analysis using cross-sectional area (CSA) analysis of myofibers strongly supported this notion; the leftward shift in myofiber size

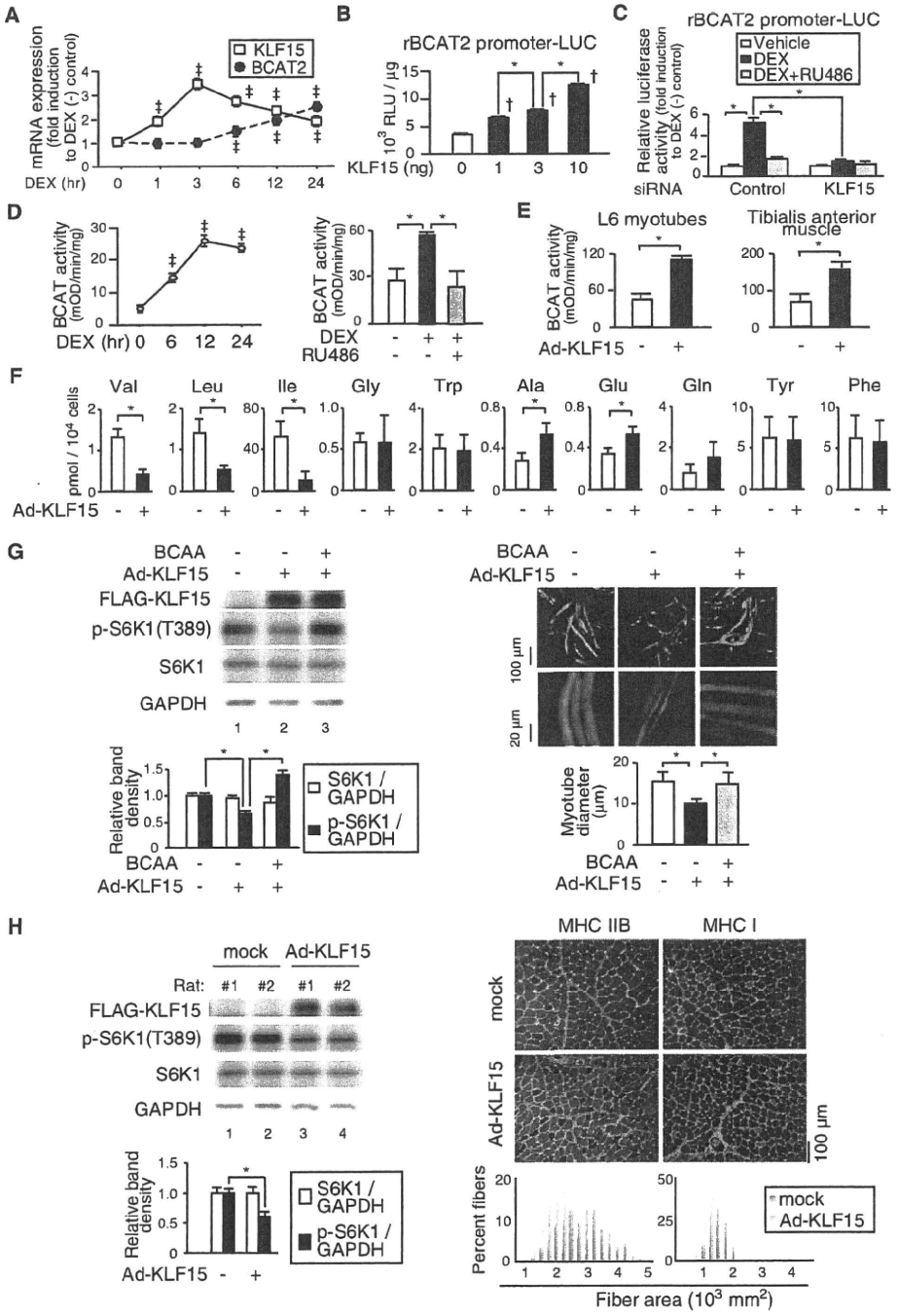

Figure 4. KLF15-Mediated Modulation of BCAA Metabolism and Myofiber Size

(A) Time course of mRNA expression of KLF15 and BCAT2 in rat gastrocnemius after intraperitoneal DEX-injection (n = 5).

(B) KLF15-dependent activation of rat BCAT2 promoter-reporter gene expression in L6 myoblasts (n = 5).

(C) Diminished GR-dependent activation of rat BCAT2 promoter-reporter gene by knockdown of KLF15 in L6 myoblasts (n = 5).

(D) GR-dependent activation of BCAT activity in rat gastrocnemius. Rats were treated with RU486 and/or DEX for the indicated time periods (left) or 6 hr (right) and subjected to BCAT activity measurement as described in the Supplemental Information (n = 5).

(E) KLF15-dependent activation of BCAT activity (n = 5).

(F) Effects of ectopic KLF15 on intracellular amino acid concentrations. L6 myotubes were infected with Ad-KLF15 for 2 days, cultured in amino acid-deprived DMEM for 24 hr, and subjected to quantification of intracellular amino acids as described in the Supplemental Information (n = 3).

(G) Effects of KLF15 and BCAA on mTOR activity and myotube diameter. C2C12 myotubes were infected with GFP-expressing adenovirus and Ad-KLF15 for 2 days and further cultured in amino acid-deprived DMEM supplemented with or without 10 mM BCAA cocktail for 24 hr. Left, representative immunoblots

was observed in the DEX group, but not in the DEX plus BCAA group. In contrast, there was no significant difference in the size of slow type I fibers among the three treatment groups. Moreover, the therapeutic effects of BCAA were inhibited by rapamycin (Figures 7B–7E). Therefore, we conclude that the administration of BCAA elicits mTOR activation and intervenes in GR-dependent catabolic transcriptional regulation to ameliorate DEX-induced muscle atrophy.

DISCUSSION

In skeletal muscle, we suggested that GR activates a secondary transcription network driven by KLF15; that the promoter regions of atrogin-1 and MuRF1 contain KLF15 binding sites as well as those of FoxOs; and that KLF15 induces the expression of these atrogenes. Although the molecular mechanism remains elusive, the functional cooperativity of GR, FoxOs, and KLF15 in the expression of the atrogenes may represent the molecular basis for the involvement of GR in muscle atrophy associated with a number of pathological conditions including diabetes and sepsis. From the metabolic viewpoint, these GR-driven transcriptional cascades appear to be relevant for providing rapid and integrated cues toward muscle breakdown and nutrient supply from muscle to other organs, i.e., to the liver, under stressful conditions associated with excess levels of glucocorticoids.

BCAT2 catalyzes the initial step for BCAA degradation, and BCAT2 activity is a critical determinant of cellular BCAA content in skeletal muscle; mice with systemic inactivation of BCAT2 gene are reported to have approximately ten times or higher concentrations of plasma BCAA (She et al., 2007). We demonstrated that BCAA content was decreased with a reciprocal increase in alanine levels in L6 myotubes after the exogenous expression of KLF15 (Figure 4F). Although it is generally known that BCAA is supplied via protein breakdown during skeletal muscle atrophy (Wagenmakers, 1998; Yu et al., 2010), it was reported that net increase in muscle BCAA concentrations after glucocorticoid treatment (~150% increase compared to control) were strikingly lower than those of diabetic rats (~400% increase compared to control) (Aftring et al., 1988; Hundal et al., 1991). This difference in BCAA concentrations is most likely to be due to increased BCAT2 activity in glucocorticoid-treated rats. The glucocorticoid-driven GR-KLF15-BCAT2 axis may negatively modulate the intracellular availability of BCAA and result in a negative impact on mTOR function in skeletal muscle. Indeed, exogenous KLF15 increased mRNA expression of the atrogenes and BCAT2 and decreased mTOR activity and BCAA concentrations in cultured myotubes (Figures 4E–4G). Moreover, the introduction of KLF15 decreased myofiber size in cultured myotubes and caused atrophy in the tibialis anterior muscle, even in the absence of glucocorticoids (Figures 4G and 4H). Therefore, we may conclude that KLF15 is a crucial GR target gene acting as a catabolic modulator of skeletal muscle.

In addition to the KLF15-BCAT2 axis, it should be noted that a number of glucocorticoid-induced products can repress mTOR activity in skeletal muscle cells. Among others, myostatin (Ma et al., 2001; Gilson et al., 2007) and REDD1 (Figure S1) (DeYoung et al., 2008) are direct targets of GR. Moreover, atrogin-1 was recently reported to inhibit S6K1 activity via eIF3f (Csibi et al., 2010). Therefore, it is likely that the mTOR system is negatively regulated by a variety of factors in the presence of excess glucocorticoids in a distinct fashion. Given that the glucocorticoid-GR axis is a major catabolic regulator for homeostatic control (Munck et al., 1984), this multimodal repression of mTOR via the GR axis appears to be rational. In any case, this type of negative mTOR modulation is not reported in other types of muscle atrophy, and may be a striking feature in glucocorticoid-induced muscle atrophy. Interestingly, muscle-specific inactivation of mTOR was reported to exacerbate the myopathic features of type I and type II fiber-rich muscles in a distinct fashion; type I fiber-rich muscles showed prominent dystrophic features with less impact on muscle mass and CSA compared to type II fiber-rich muscles, and a decrease in muscle mass and CSA are characteristic of type II fiber-rich muscles with less dystrophic appearance (Bentzinger et al., 2008; Risson et al., 2009). Therefore, we speculate that type II fiber-rich glycolytic muscles have an evolutionally preserved role for the storage of nutrients under the control of the glucocorticoid-GR axis and that the GR-triggered gene expression program is a purposeful and efficient compensatory mechanism for nutrient supply from those muscles.

An important question is how the GR-driven proteolytic cascades can be shut down when necessary in skeletal muscle. We clearly demonstrated that mTOR activation negatively modulated GR-mediated transcription. Given that the effect of mTOR is rapamycin sensitive, the involvement of mTORC1 is strongly indicated in this interaction. The role of the mTOR pathway in the determination of glucocorticoid sensitivity has not yet been highlighted, except in certain hematologic malignancies (Beesley et al., 2009; Gu et al., 2008; Yan et al., 2006a). It was postulated that the treatment of cultured cells with FK506 or rapamycin enhances glucocorticoid-inducible reporter gene expression, most possibly via their interaction with heat shock proteins and the promotion of the ligand-dependent nuclear entry of GR (Ning and Sanchez, 1993). In contrast, we documented that rapamycin, without any alteration in the cytoplasmic-nuclear distribution of GR, increased GR recruitment onto the promoter (Figures 5E and 5F), and these effects were not reproduced by FK506 (data not shown).

and quantified band densities of S6K1 and p-S6K1(T389) relative to GAPDH ($n = 5$). Right, representative fluorescent microscopic images of the myotubes and quantified diameters of the myotubes ($500 < n < 510$).

(H) Effects of ectopic KLF15 expression on mTOR activity and myofiber cross-sectional area (CSA) in rat tibialis anterior. Left, representative immunoblots and quantified band densities ($n = 5$). Right, immunostaining for type IIB myosin heavy chain (MHC IIB, red in left photographs), type I myosin heavy chain (MHC I, red in right photographs), and type IV collagen (green) of transverse cryosections. CSA distribution of MHC IIB fibers (left) and MHC I fibers (right) are presented as frequency histograms ($500 < n < 510$).

(A–H) Error bars show SD. $^{*}p < 0.05$, $^{\ddagger}p < 0.05$ versus vehicle-treated rats. $^{\dagger}p < 0.05$ versus mock-transfected cells.

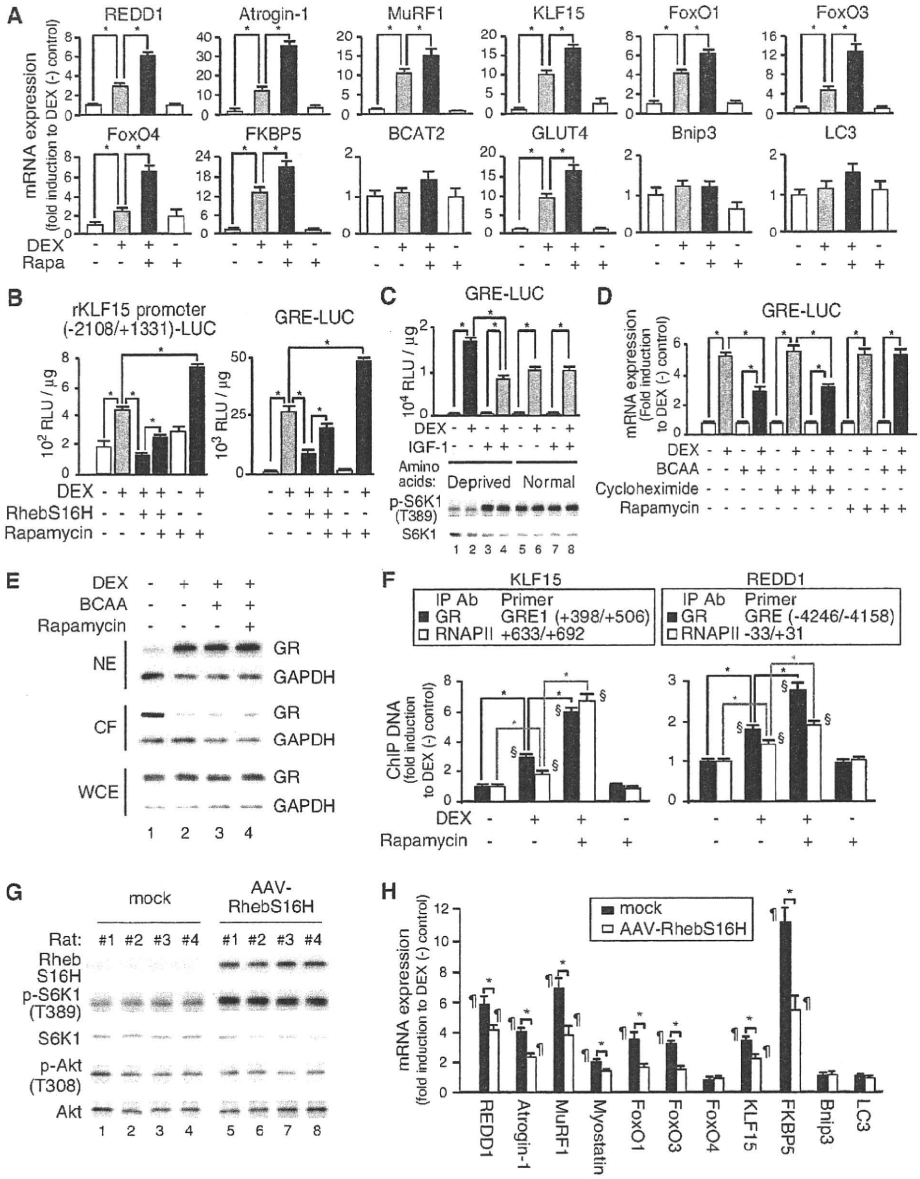

Figure 5. Negative Regulation of GR-Mediated Transcription by mTOR

(A) qRT-PCR analysis of L6 myotubes treated with DEX and rapamycin (Rapa) for 24 hr.

(B) Attenuation of GR-dependent reporter gene expression by mTOR. L6 myoblasts were transfected with rKLF15 promoter-LUC or GRE-LUC, with or without the expression plasmid for a constitutive active Rheb (RhebS16H), and treated with DEX and rapamycin for 18 hr.

(C) Effects of IGF-1 on mTOR activity and GR-dependent reporter gene expression. L6 myoblasts were transfected with GRE-LUC and cultured in amino acid-deprived DMEM (lanes 1–4) or normal DMEM (lanes 5–8) in the presence or absence of IGF-1 and/or DEX for 9 hr. Top, luciferase activities. Bottom, representative immunoblots.

(D) Effects of DEX, BCAA, cycloheximide, and rapamycin on GR-dependent reporter gene expression. L6 myoblasts were transfected with GRE-LUC and cultured in amino acid-deprived DMEM in the presence or absence of 10 mM BCAA cocktail, cycloheximide, rapamycin, and DEX for 6 hr.

(E) Effects of DEX, BCAA, and rapamycin on protein levels and subcellular localization of GR. L6 myotubes were cultured in amino acid-deprived DMEM in the presence or absence of DEX, 10 mM BCAA cocktail, and rapamycin for 30 min. Representative immunoblots of the nuclear extracts (NE), cytoplasmic fractions (CF), and whole-cell extracts (WCE) are shown (n = 3).

(F) Effects of rapamycin on DEX-dependent recruitment of GR onto target gene promoters. L6 myotubes were treated with 1 µM DEX and rapamycin for 2 hr (for KLF15) or 20 min (for REDD1) and processed for ChIP assays.

(G and H) Effects of ectopic expression of RhebS16H on mTOR activity and DEX-mediated mRNA expression. AAV-RhebS16H was infected to rat tibialis anterior for 7 days. (G) Representative immunoblots (n = 7). (H) qRT-PCR analysis of the muscles from the rats 6 hr after intraperitoneal injection with DEX.

(A–D, F, and H) Error bars show SD (n = 5). *$p < 0.05$, §$p < 0.05$ versus ChIP with normal IgG, ¶$p < 0.05$ versus vehicle-treated rats.

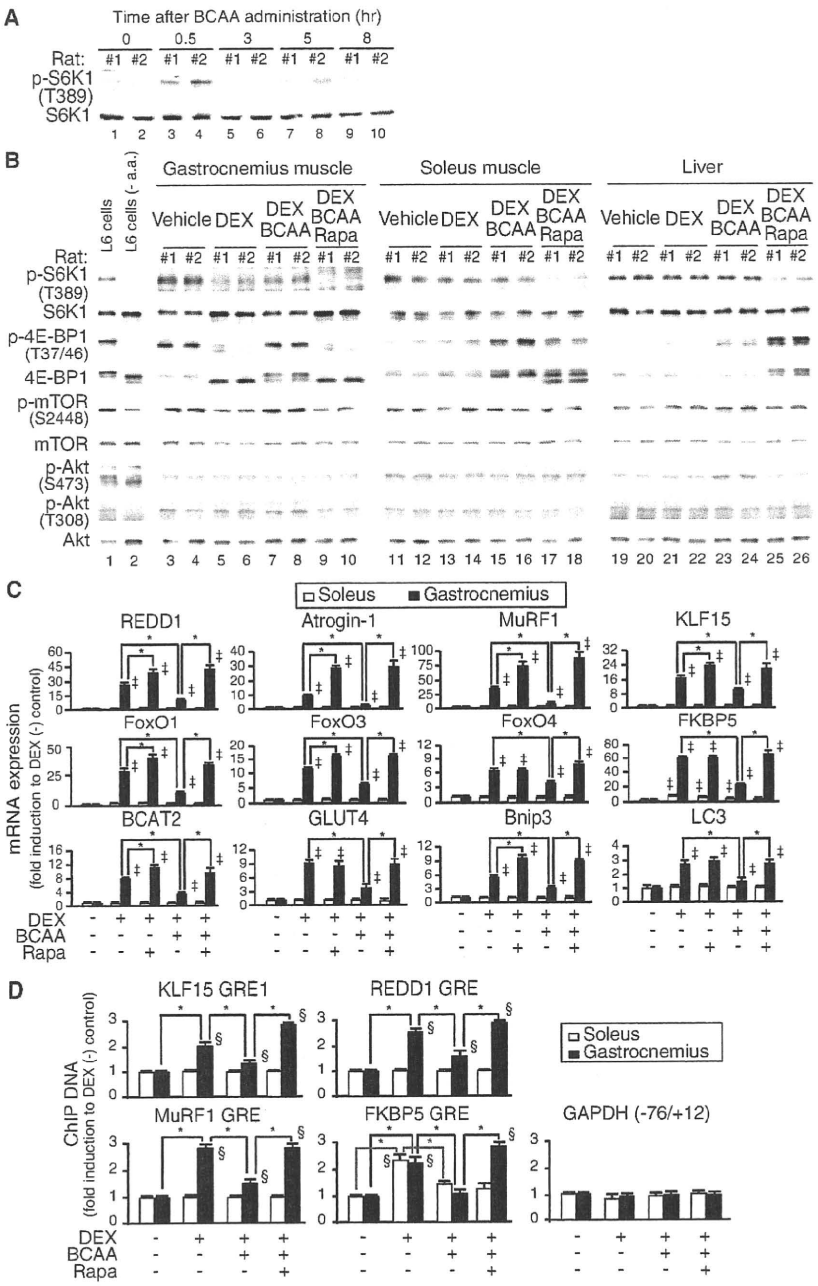

Figure 6. In Vivo Activation of mTOR and Attenuation of GR-Mediated Transcription after Programmed Administration of BCAA

(A) Time course of mTOR activity in rat gastrocnemius after BCAA administration. Representative immunoblots are shown (n = 5).

(B–D) Effects of DEX, BCAA, and rapamycin on mTOR activity; mRNA expression of atrophy-related genes; and GR recruitment onto the target gene promoters. Rats were treated with DEX, BCAA cocktail, and rapamycin for 5 days as described in the Supplemental Information. (B) Representative immunoblots (n = 17). L6 myotubes cultured in normal DMEM and in amino acid-deprived DMEM (−a.a.) for 1 hr were served as controls. (C) mRNA expression of atrophy-related genes. (D) Recruitment of GR onto its target genes. ChIP was performed using anti-GR antibody.

(C and D) Error bars show SD (n = 17). *$p < 0.05$, †$p < 0.05$ versus vehicle-treated rats, §$p < 0.05$ versus ChIP with normal IgG.

In skeletal muscle, this nutrition sensor-driven inhibition of GR function may be one of the mechanisms by which nutrients modulate the internal cellular milieu. Intriguingly, GR-mediated transcription was not repressed by insulin/IGF-1 under normal culture conditions, but did so when amino acids were deprived from the culture media (Figure 5C). This indicates that mTOR may be constitutively activated to a certain extent by nutrients and growth factors to protect cells from GR-driven catabolism in skeletal muscle. Under fasting conditions, however, blood concentrations of insulin/IGF-1 are low, and glucocorticoids may be allowed to efficiently drive the catabolic atrophy program for nutrient supply. Thus, our hypothesis may provide an insight into how muscle cells critically determine their volume after sensing endocrine hormones and the nutritional conditions for homeostatic regulation. In this context, GR-mTOR crosstalk might be a key for creating an interdisciplinary research area that bridges nutrition and medicine.

Therefore, the mTOR-mediated inhibition of GR in skeletal muscle is likely to be due not to the modulation of its chaperone activity but to its intervention in the access of GR to target DNA. It is becoming apparent that mTOR is intimately involved with the transcriptional apparatus in concert with a variety of transcription factors and cofactors (Cunningham et al., 2007). Since mTOR is reported to dock in the nucleus in association with, for example, PML (Bernardi et al., 2006), it would be of particular interest to identify such a factor that tethers GR and mTOR in the nucleus.

The biochemical rationale for the usage of BCAA as a therapeutic tool in glucocorticoid-induced muscle atrophy is that BCAA increases the association between Rheb and mTOR and, at least in part, mimics the effect of Rheb overexpression (Sancak et al., 2010). In our model, BCAA administration repressed mRNA expression of almost all GR-regulated genes (Figure 6C). ChIP analysis strongly supported the notion that BCAA administration inhibited GR recruitment onto the promoters of its target genes (Figure 6D). Moreover, these effects of BCAA were efficiently counteracted by rapamycin.

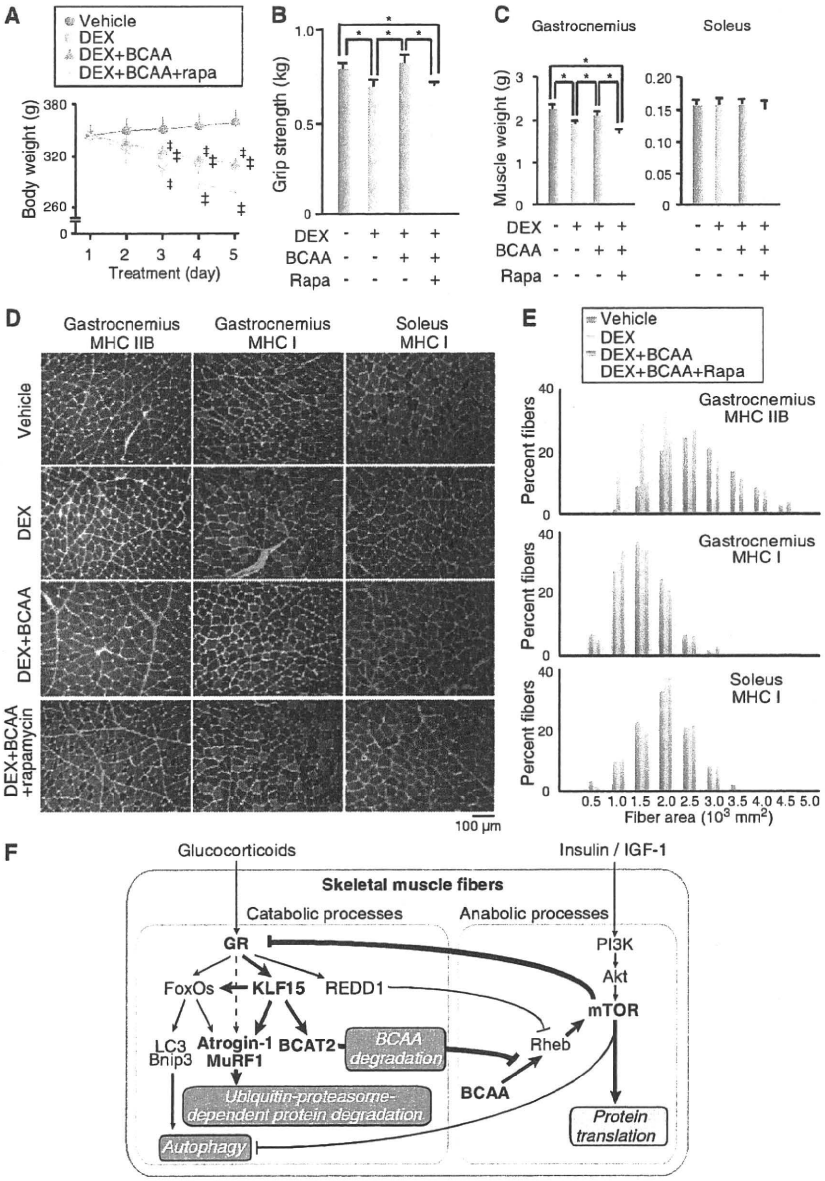

Figure 7. Restoration of Muscle Fiber Mass and Strength by mTOR Activation in DEX-Induced Skeletal Muscle Atrophy Model

(A–E) Effects of DEX, BCAA, and rapamycin on body weight (A), grip strength of forearms (B), muscle weight (C), muscle pathology (D), and CSA of skeletal muscle fiber (E). Rats were treated with DEX, BCAA, and rapamycin for 5 days as described in the Supplemental Information. (A) Time course of body weight ($n = 15$). (B) Grip strength of forearms at 5 hr after DEX injection on the day 5 ($47 < n < 51$). (C) Weight of gastrocnemius and soleus at 6 hr after DEX injection on the day 5 ($n = 15$). (D) Immunostaining for MHC IIB (red in left photographs), MHC I (red in middle and right photographs), and type IV collagen (green) of transverse cryosections. (E) CSA distribution of MHC IIB fibers (gastrocnemius) and MHC I fibers (gastrocnemius and soleus) presented as frequency histograms ($500 < n < 510$). (F) Schematic model of mutual crosstalk between catabolic processes and anabolic processes in skeletal muscle.

(A–C) Error bars show SD (A and C) or SEM (B). $^{*}p < 0.05$, $^{\ddagger}p < 0.05$ versus vehicle-treated rats.

Therefore, we are convinced that the therapeutic effects of BCAA could, at least in part, be ascribed to GR inhibition by the BCAA-mediated activation of mTOR. BCAA administration also resulted in the decreased mRNA expression of autophagy-related genes (Figure 6C), indicating that this therapeutic regimen repressed the vicious circuit connecting the initial induction of GR-triggered gene expression to degradation and atrophy. Of course, we cannot rule out other mechanisms for the effects of BCAA, including the non-GR-mediated repression of atrophy and/or autophagy, and further studies are clearly needed to clarify this issue.

There are conflicting results concerning the biological effects of BCAA, e.g., the overactivation of amino acid-dependent mTOR-mediated signaling can lead to the inhibition of the proximal part of the insulin signaling pathway (Um et al., 2006). Moreover, in obese humans, BCAA in association with a high-fat diet is linked to the elevation of insulin resistance (Newgard et al., 2009). On the other hand, it is suggested that an increase in type II fibers in obese mice may reduce fat mass and improve metabolic parameters (Izumiya et al., 2008). Therefore, it is necessary, for the validation of BCAA therapy, to evaluate the influence of long-term BCAA administration on various metabolic parameters.

In conclusion, we revealed that GR and mTOR act as catabolic and anabolic liaisons for skeletal muscle metabolism, respectively, and these molecules interact with each other at multiple levels. This issue would be of particular importance to understand the molecular mechanism underlying the regulation of the volume and metabolism of muscle and for the development of treatments for glucocorticoid-induced and wasting disorder-related skeletal muscle atrophy.

EXPERIMENTAL PROCEDURES

Rats

All animal experiments were approved by the institutional committee and conducted according to the institutional ethical guidelines for animal experiments. Rapamycin, RU486, the BCAA cocktail, and DEX administration were performed as described in the Supplemental Information. Excised tissues were snap frozen in isopentane cooled by liquid nitrogen, and crushed using Cryo-Press (Microtec, Funabashi, Japan) prefrozen in liquid nitrogen, or processed to serial 10 μm transverse cryostat sections.

Cell Culture

L6 rat myoblasts, C2C12 mouse myoblasts, and COS-7 cells were obtained from American Type Culture Collection (Manassas, VA) and maintained in DMEM supplemented with 10% fetal bovine serum (Invitrogen, Carlsbad, CA). Culture conditions for myotube formation, drug treatment, and amino acids deprivation are described in the Supplemental Information.

In Silico Promoter Analysis

Putative FoxO1- and FoxO3-binding sequences, as well as putative GREs which are conserved between rat and human genomes, were searched for in the genomic regions (−5000 to +2000) of KLF15, REDD1, atrogin-1, and MuRF1 using rVISTA 2.0 as described in the Supplemental Information. KLF15-binding sequences (see the Supplemental Information) were searched for in the promoters of rat atrogin-1 (−4141 to +1191) and MuRF1 (−3223 to +1547) genes.

Chromatin Immunoprecipitation Assay

Cells or crushed tissues were treated with 1% formaldehyde in PBS for 10 min at 37°C, incubated in 125 mM glycine for 5 min, resuspended in buffer S (50 mM Tris [pH 8.0], 1% SDS, 10 mM EDTA) supplemented with 1 mM DTT, 100 nM MG132, and protease and phosphatase inhibitor cocktail (Nacalai Tesque, Kyoto, Japan), and incubated at 10°C for 10 min. Samples were sheared to an average size of 500 bp by sonication. Lysates corresponding to 2×10^6 cells or 200 mg of crushed tissues were diluted 10-fold in buffer D (0.01% SDS, 1.1% Triton X-100, 1.2 mM EDTA, 16.7 mM Tris [pH 8.1], 167 mM NaCl) supplemented with 100 nM MG132, and protease and phosphatase inhibitor cocktail, and incubated with 5 μg of antibodies listed in the Supplemental Information at 4°C for 18 hr. Protein A or G agarose/salmon sperm DNA (Millipore, Billerica, MA) was added and further incubated at 4°C for 1 hr. Precipitated DNA were quantified as described in the Supplemental Information.

Indirect Immunofluorescent Staining and Fluorescence Imaging

Muscle cryosections were treated with 0.1% Triton X-100, blocked with 5% goat serum/1% BSA in PBS, and incubated with antibodies listed in the Supplemental Information. After washing with PBS, specimens were incubated with secondary antibodies labeled with Alexa Fluor 488 or Alexa Fluor 568 (Invitrogen, 1:1000) and analyzed as described in the Supplemental Information. For imaging cultured myotubes, GFP was expressed in myotubes by infecting 10 multiplicity of infection of Ax1CAgfp (RIKEN DNA Bank, Tsukuba, Japan).

Statistical Analysis

Data were analyzed with Student's t test for unpaired data. P values below 0.05 were considered statistically significant. Graphs represent means ± SD or means ± SEM as specified in each figure legend.

SUPPLEMENTAL INFORMATION

Supplemental Information include one figure, Supplemental Experimental Procedures, and Supplemental References and can be found with this article at doi:10.1016/j.cmet.2011.01.001.

ACKNOWLEDGMENTS

This work was supported by Grants-in-Aid for Scientific Research, (to H.T., N.S., and N.Y.) and by grants from the Ministry of Health, Labour, and Welfare and from Japan Science and Technology Agency, Japan (to H.T.). Y.T., S.N., and K.T. are employees of Ajinomoto Pharmaceutical Company.

Received: June 17, 2010
Revised: October 14, 2010
Accepted: December 30, 2010
Published: February 1, 2011

REFERENCES

Aftring, R.P., Miller, W.J., and Buse, M.G. (1988). Effects of diabetes and starvation on skeletal muscle branched-chain alpha-keto acid dehydrogenase activity. Am. J. Physiol. *254*, E292–E300.

Beesley, A.H., Firth, M.J., Ford, J., Weller, R.E., Freitas, J.R., Perera, K.U., and Kees, U.R. (2009). Glucocorticoid resistance in T-lineage acute lymphoblastic leukaemia is associated with a proliferative metabolism. Br. J. Cancer *100*, 1926–1936.

Bentzinger, C.F., Romanino, K., Cloetta, D., Lin, S., Mascarenhas, J.B., Oliveri, F., Xia, J., Casanova, E., Costa, C.F., Brink, M., et al. (2008). Skeletal muscle-specific ablation of raptor, but not of rictor, causes metabolic changes and results in muscle dystrophy. Cell Metab. *8*, 411–424.

Bernardi, R., Guernah, I., Jin, D., Grisendi, S., Alimonti, A., Teruya-Feldstein, J., Cordon-Cardo, C., Simon, M.C., Rafii, S., and Pandolfi, P.P. (2006). PML inhibits HIF-1alpha translation and neoangiogenesis through repression of mTOR. Nature *442*, 779–785.

Csibi, A., Cornille, K., Leibovitch, M.P., Poupon, A., Tintignac, L.A., Sanchez, A.M., and Leibovitch, S.A. (2010). The translation regulatory subunit eIF3f controls the kinase-dependent mTOR signaling required for muscle differentiation and hypertrophy in mouse. PLoS ONE *5*, e8994. 10.1371/journal.pone.0008994.

Cunningham, J.T., Rodgers, J.T., Arlow, D.H., Vazquez, F., Mootha, V.K., and Puigserver, P. (2007). mTOR controls mitochondrial oxidative function through a YY1-PGC-1alpha transcriptional complex. Nature *450*, 736–740.

DeYoung, M.P., Horak, P., Sofer, A., Sgroi, D., and Ellisen, L.W. (2008). Hypoxia regulates TSC1/2-mTOR signaling and tumor suppression through REDD1-mediated 14-3-3 shuttling. Genes Dev. *22*, 239–251.

Evans, R.M. (2005). The nuclear receptor superfamily: a rosetta stone for physiology. Mol. Endocrinol. *19*, 1429–1438.

Fisch, S., Gray, S., Heymans, S., Haldar, S.M., Wang, B., Pfister, O., Cui, L., Kumar, A., Lin, Z., Sen-Banerjee, S., et al. (2007). Kruppel-like factor 15 is a regulator of cardiomyocyte hypertrophy. Proc. Natl. Acad. Sci. USA *104*, 7074–7079.

Gilson, H., Schakman, O., Combaret, L., Lause, P., Grobet, L., Attaix, D., Ketelslegers, J.M., and Thissen, J.P. (2007). Myostatin gene deletion prevents glucocorticoid-induced muscle atrophy. Endocrinology *148*, 452–460.

Glass, D.J. (2003). Signalling pathways that mediate skeletal muscle hypertrophy and atrophy. Nat. Cell Biol. *5*, 87–90.

Gray, S., Wang, B., Orihuela, Y., Hong, E.G., Fisch, S., Haldar, S., Cline, G.W., Kim, J.K., Peroni, O.D., Kahn, B.B., and Jain, M.K. (2007). Regulation of gluconeogenesis by Krüppel-like factor 15. Cell Metab. *5*, 305–312.

Gu, L., Gao, J., Li, Q., Zhu, Y.P., Jia, C.S., Fu, R.Y., Chen, Y., Liao, Q.K., and Ma, Z. (2008). Rapamycin reverses NPM-ALK-induced glucocorticoid resistance in lymphoid tumor cells by inhibiting mTOR signaling pathway, enhancing G1 cell cycle arrest and apoptosis. Leukemia *22*, 2091–2096.

Hoffman, E.P., and Nader, G.A. (2004). Balancing muscle hypertrophy and atrophy. Nat. Med. *10*, 584–585.

Hu, Z., Wang, H., Lee, I.H., Du, J., and Mitch, W.E. (2009). Endogenous glucocorticoids and impaired insulin signaling are both required to stimulate muscle wasting under pathophysiological conditions in mice. J. Clin. Invest. *119*, 3059–3069.

Hundal, H.S., Babij, P., Taylor, P.M., Watt, P.W., and Rennie, M.J. (1991). Effects of corticosteroid on the transport and metabolism of glutamine in rat skeletal muscle. Biochim. Biophys. Acta *1092*, 376–383.

Izumiya, Y., Hopkins, T., Morris, C., Sato, K., Zeng, L., Viereck, J., Hamilton, J.A., Ouchi, N., LeBrasseur, N.K., and Walsh, K. (2008). Fast/Glycolytic muscle fiber growth reduces fat mass and improves metabolic parameters in obese mice. Cell Metab. *7*, 159–172.

Ma, K., Mallidis, C., Artaza, J., Taylor, W., Gonzalez-Cadavid, N., and Bhasin, S. (2001). Characterization of 5′-regulatory region of human myostatin gene: regulation by dexamethasone in vitro. Am. J. Physiol. Endocrinol. Metab. *281*, E1128–E1136.

Mammucari, C., Milan, G., Romanello, V., Masiero, E., Rudolf, R., Del Piccolo, P., Burden, S.J., Di Lisi, R., Sandri, C., Zhao, J., et al. (2007). FoxO3 controls autophagy in skeletal muscle in vivo. Cell Metab. *6*, 458–471.

Matthews, S.E. (1999). Proteins and amino acids. In Modern Nutrition and Health and Diseases, 9th ed., M.E. Shils, J.A. Olson, M. Shike, and A.C. Ross, eds. (Baltimore: Williams & Wilkins), pp. 11–48.

Meijsing, S.H., Pufall, M.A., So, A.Y., Bates, D.L., Chen, L., and Yamamoto, K.R. (2009). DNA binding site sequence directs glucocorticoid receptor structure and activity. Science *324*, 407–410.

Menconi, M., Fareed, M., O'Neal, P., Poylin, V., Wei, W., and Hasselgren, P.O. (2007). Role of glucocorticoids in the molecular regulation of muscle wasting. Crit. Care Med. *35*, S602–S608.

Mizushima, N., Levine, B., Cuervo, A.M., and Klionsky, D.J. (2008). Autophagy fights disease through cellular self-digestion. Nature *451*, 1069–1075.

Moresi, V., Williams, A.H., Meadows, E., Flynn, J.M., Potthoff, M.J., McAnally, J., Shelton, J.M., Backs, J., Klein, W.H., Richardson, J.A., et al. (2010). Myogenin and class II HDACs control neurogenic muscle atrophy by inducing E3 ubiquitin ligases. Cell *143*, 35–45.

Munck, A., Guyre, P.M., and Holbrook, N.J. (1984). Physiological functions of glucocorticoids in stress and their relation to pharmacological actions. Endocr. Rev. *5*, 25–44.

Newgard, C.B., An, J., Bain, J.R., Muehlbauer, M.J., Stevens, R.D., Lien, L.F., Haqq, A.M., Shah, S.H., Arlotto, M., Slentz, C.A., et al. (2009). A branched-chain amino acid-related metabolic signature that differentiates obese and lean humans and contributes to insulin resistance. Cell Metab. *9*, 311–326.

Ning, Y.M., and Sanchez, E.R. (1993). Potentiation of glucocorticoid receptor-mediated gene expression by the immunophilin ligands FK506 and rapamycin. J. Biol. Chem. *268*, 6073–6076.

Risson, V., Mazelin, L., Roceri, M., Sanchez, H., Moncollin, V., Corneloup, C., Richard-Bulteau, H., Vignaud, A., Baas, D., Defour, A., et al. (2009). Muscle inactivation of mTOR causes metabolic and dystrophin defects leading to severe myopathy. J. Cell Biol. *187*, 859–874.

Sancak, Y., Bar-Peled, L., Zoncu, R., Markhard, A.L., Nada, S., and Sabatini, D.M. (2010). Ragulator-Rag complex targets mTORC1 to the lysosomal surface and is necessary for its activation by amino acids. Cell *141*, 290–303.

Sandri, M. (2008). Signaling in muscle atrophy and hypertrophy. Physiology (Bethesda) *23*, 160–170.

Sandri, M., Sandri, C., Gilbert, A., Skurk, C., Calabria, E., Picard, A., Walsh, K., Schiaffino, S., Lecker, S.H., and Goldberg, A.L. (2004). Foxo transcription factors induce the atrophy-related ubiquitin ligase atrogin-1 and cause skeletal muscle atrophy. Cell *117*, 399–412.

Schakman, O., Gilson, H., and Thissen, J.P. (2008). Mechanisms of glucocorticoid-induced myopathy. J. Endocrinol. *197*, 1–10.

Sengupta, S., Peterson, T.R., and Sabatini, D.M. (2010). Regulation of the mTOR complex 1 pathway by nutrients, growth factors, and stress. Mol. Cell *40*, 310–322.

She, P., Reid, T.M., Bronson, S.K., Vary, T.C., Hajnal, A., Lynch, C.J., and Hutson, S.M. (2007). Disruption of BCATm in mice leads to increased energy expenditure associated with the activation of a futile protein turnover cycle. Cell Metab. *6*, 181–194.

Stitt, T.N., Drujan, D., Clarke, B.A., Panaro, F., Timofeyva, Y., Kline, W.O., Gonzalez, M., Yancopoulos, G.D., and Glass, D.J. (2004). The IGF-1/PI3K/Akt pathway prevents expression of muscle atrophy-induced ubiquitin ligases by inhibiting FOXO transcription factors. Mol. Cell *14*, 395–403.

Suzuki, N., Motohashi, N., Uezumi, A., Fukada, S., Yoshimura, T., Itoyama, Y., Aoki, M., Miyagoe-Suzuki, Y., and Takeda, S. (2007). NO production results in suspension-induced muscle atrophy through dislocation of neuronal NOS. J. Clin. Invest. *117*, 2468–2476.

Um, S.H., D'Alessio, D., and Thomas, G. (2006). Nutrient overload, insulin resistance, and ribosomal protein S6 kinase 1, S6K1. Cell Metab. *3*, 393–402.

Waddell, D.S., Baehr, L.M., van den Brandt, J., Johnsen, S.A., Reichardt, H.M., Furlow, J.D., and Bodine, S.C. (2008). The glucocorticoid receptor and FOXO1 synergistically activate the skeletal muscle atrophy-associated MuRF1 gene. Am. J. Physiol. Endocrinol. Metab. *295*, E785–E797.

Wagenmakers, A.J. (1998). Protein and amino acid metabolism in human muscle. Adv. Exp. Med. Biol. *441*, 307–319.

Wang, H., Kubica, N., Ellisen, L.W., Jefferson, L.S., and Kimball, S.R. (2006). Dexamethasone represses signaling through the mammalian target of rapamycin in muscle cells by enhancing expression of REDD1. J. Biol. Chem. *281*, 39128–39134.

Yan, H., Frost, P., Shi, Y., Hoang, B., Sharma, S., Fisher, M., Gera, J., and Lichtenstein, A. (2006a). Mechanism by which mammalian target of rapamycin inhibitors sensitize multiple myeloma cells to dexamethasone-induced apoptosis. Cancer Res. *66*, 2305–2313.

Yoshikawa, N., Nagasaki, M., Sano, M., Tokudome, S., Ueno, K., Shimizu, N., Imoto, S., Miyano, S., Suematsu, M., Fukuda, K., et al. (2009). Ligand-based gene expression profiling reveals novel roles of glucocorticoid receptor in cardiac metabolism. Am. J. Physiol. Endocrinol. Metab. *296*, E1363–E1373.

Yu, L., McPhee, C.K., Zheng, L., Mardones, G.A., Rong, Y., Peng, J., Mi, N., Zhao, Y., Liu, Z., Wan, F., et al. (2010). Termination of autophagy and reformation of lysosomes regulated by mTOR. Nature *465*, 942–946.

Zhao, J., Brault, J.J., Schild, A., Cao, P., Sandri, M., Schiaffino, S., Lecker, S.H., and Goldberg, A.L. (2007). FoxO3 coordinately activates protein degradation by the autophagic/lysosomal and proteasomal pathways in atrophying muscle cells. Cell Metab. *6*, 472–483.

EXPERIMENTAL CELL RESEARCH 316 (2010) 3087–3092

available at www.sciencedirect.com

ScienceDirect

www.elsevier.com/locate/yexcr

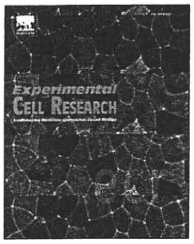

Review

Gene therapy for muscle disease

*Yuko Miyagoe-Suzuki, Shin'ichi Takeda**

Department of Molecular Therapy, National Institute of Neuroscience, National Center of Neurology and Psychiatry, 4-1-1 Ogawa-higashi, Kodaira, Tokyo 187-8502, Japan

ARTICLE INFORMATION

Article Chronology:
Received 25 March 2010
Revised version received 13 May 2010
Accepted 17 May 2010
Available online 24 May 2010

Keywords:
Dystrophin
Duchenne muscular dystrophy (DMD)
Recombinant adenoassociated viral (AAV)
Exon skipping
Antisense oligonucleotide
Gene therapy

ABSTRACT

The molecular mechanisms of Duchenne muscular dystrophy (DMD) have been extensively investigated since the discovery of the dystrophin gene in 1986. Nonetheless, there is currently no effective treatment for DMD. Recent reports, however, indicate that adenoassociated viral (AAV) vector-mediated transfer of a functional dystrophin cDNA into the affected muscle is a promising strategy. In addition, antisense-mediated exon skipping technology has been emerging as another promising approach to restore dystrophin expression in DMD muscle. Ongoing clinical trials show restoration of dystrophin in DMD patients without serious side effects. Here, we summarize the recent progress in gene therapy, with an emphasis on exon skipping for DMD.

Contents

* *Corresponding author.* Fax: +81 42 346 1750.
E-mail address: takeda@ncnp.go.jp (S. Takeda).

0014-4827/$ – see front matter © 2010 Elsevier Inc. All rights reserved.
doi:10.1016/j.yexcr.2010.05.022

Introduction

Muscular dystrophies are heterogeneous genetic disorders, characterized by progressive degeneration and weakness of the skeletal and cardiac muscles. DMD is severe and the most common type of muscular dystrophy; worldwide, approximately one in every 3500 boys born is afflicted with DMD.

The *DMD* gene is the largest known gene in humans, comprising over 79 exons, with a coding sequence of 11 kb and spans no less than 2.3 Mb of genomic DNA. DMD is caused by deletion (65%), duplication (15%), or nonsense and other small mutations (20%) in the *DMD* gene, all of which disrupt the open reading frame [1].

The *DMD* gene encodes dystrophin, which is located beneath the sarcolemma, assembles the dystrophin–glycoprotein complex at the sarcolemma, and links the internal cytoplasmic actin filament network and extracellular matrix, providing physical strength to muscle fibers [2]. At present, there is no effective therapy to stop the lethal progression of the disease, but several therapeutic approaches hold great potential. Here we focus on gene therapy for DMD and summarize AO-mediated exon skipping technology as a most promising therapy.

Adenoassociated virus -mediated gene therapy

Updates on rAAVs

The adenoassociated virus (AAV) is a tiny single-stranded, nonpathogenic, nonreplicative DNA virus belonging to the Parvovirus family. So far, more than 12 serotypes have been identified in primates [3]. Recombinant AAV (rAAV) is a powerful tool to deliver therapeutic genes to skeletal muscle [4–6]. Even in immunologically competent mice, the expression of the exogenous gene was shown to continue for years without evoking immune responses.

Importantly, rAAV has several serotypes that show tropisms to skeletal muscle. rAAV1 and rAAV2 are commonly used for direct delivery to skeletal muscle and mainly used in local treatment. rAAV-6 [7] plus the more recently developed rAAV-8 [8,9], and rAAV-9 [10–12] are powerful in systemic delivery of the therapeutic genes via the circulation to the musculature body-wide, including the diaphragm and heart.

Limited packaging size of rAAV

rAAV has a limitation in the length of the transgene it can accommodate (less than 5.0 kb). Full-length dystrophin, which is nearly 11 kb, cannot be incorporated into an AAV vector. To overcome this limitation, truncated but functional microdystrophins with a large deletion in the central rod domain have been constructed because studies of the genotype–phenotype relationships in DMD and Becker muscular dystrophy (BMD), a milder form of muscular dystrophy with near-normal life expectancy, have suggested that the rod domain has limited function and is largely dispensable [4]. Several types of microdystrophin were administrated to *mdx* mice locally [13] or systemically [7,14–16] and ameliorated pathology and improved muscle function. To expand the packaging capacity of the AAV vector, trans-splicing (ts) of two vectors and recombination of two overlapping (ov) rAAV vectors have been tested (reviewed in Trollet et al. [4]). A hybrid dual-vector system, which combines the features of the ts and ov vectors into a single system, has been reported to work well in skeletal muscle [17].

Immunity against rAAV in dog models

Based on the improvement of pathology and muscle function due to successful AAV-mediated gene transfer into dystrophic mice, preclinical studies using dystrophic dogs [18,19] and nonhuman primates [20,21] were performed. In dogs, considerable cellular immune response was often observed [18,19,22], and transient immune suppression was needed [23]. However, there is no clear explanation of why rAAVs evoke much stronger immune responses in dogs than mice.

Clinical trials

Immunity to AAVs is also a big concern in rAAV-mediated gene therapy for DMD. First, natural AAV infection is quite common in human populations, and preexisting antibodies could block AAV vector-mediated therapy. Second, after the first injection of rAAV vectors, the second injection is known to be much less effective due to a neutralizing antibody. Indeed, clinical trials using AAV vectors suggest that immune response to the vector and/or transgene product is the most important limitation of the rAAV-mediated gene therapy. To diminish a host immune response against the transgene product, utilization of a muscle-specific promoter active in both skeletal and cardiac muscles [24,25] is desirable. Codon optimization has also been demonstrated to be effective to reduce the virus titer [26]. A phase I/II clinical trial of intramuscular delivery of microdystrophin by AAV2.5-CMV-Mini-Dystrophin was initiated in 2006 (PI: JR Mendell; Trial ID: US-679; clinicaltrials.gov identifier: NCT00428935). More information can be obtained at http://www.wiley.co.uk/genetherapy/clinical/, http://www.clinicaltrials.gov, or http://www.mda.org.

Lentiviral vector-mediated gene transfer into muscle stem cells

Lentiviral vectors have a relatively large transgene carrying capacity (7.5–9 kb), integrate into the genomes of both dividing and nondividing cells, and achieve long-term transgene expression in a wide variety of tissues including skeletal muscle. Previously, lentiviral vectors have been used to introduce a mini-dystrophin gene into mouse skeletal muscle [27]. Because the expression levels of mini-dystrophin were low after direct injection of lentiviral